



University of Dundee

Differential expression analyses on aortic tissue reveal novel genes and pathways associated with abdominal aortic aneurysm onset and progression

Temprano-Sagrera, Gerard; Soto, Begoña; Dilmé, Jaume; Peypoch, Olga; Juscafresa, Laura Calsina; Davtian, David

DOI:
[10.1101/2024.02.26.24303384](https://doi.org/10.1101/2024.02.26.24303384)

Publication date:
2024

Licence:
CC BY-NC-ND

Document Version
Early version, also known as pre-print

[Link to publication in Discovery Research Portal](#)

Citation for published version (APA):
Temprano-Sagrera, G., Soto, B., Dilmé, J., Peypoch, O., Juscafresa, L. C., Davtian, D., Nieto, L., Brown, A., Escudero, J. R., Viñuela, A., Camacho, M., & Sabater-Lleal, M. (2024). *Differential expression analyses on aortic tissue reveal novel genes and pathways associated with abdominal aortic aneurysm onset and progression*. medRxiv. <https://doi.org/10.1101/2024.02.26.24303384>

General rights

Copyright and moral rights for the publications made accessible in Discovery Research Portal are retained by the authors and/or other copyright owners and it is a condition of accessing publications that users recognise and abide by the legal requirements associated with these rights.

Take down policy

If you believe that this document breaches copyright please contact us providing details, and we will remove access to the work immediately and investigate your claim.

1 **Differential expression analyses on aortic tissue reveal novel genes and pathways associated**
2 **with abdominal aortic aneurysm onset and progression**

3 Gerard Temprano-Sagrera MSc (gtemprano@santpau.cat)¹, Begoña Soto MD PhD
4 (bsoto@santpau.cat)^{1,2}, Jaume Dilmé MD PhD (jdilme@santpau.cat)^{1,2,3}, Olga Peypoch MD
5 (opeypoch@santpau.cat)^{1,2}, Laura Calsina Juscafresa MD PhD (lcalsina@psmar.cat)^{4,5}, David
6 Davtian PhD⁶ (2400580@dundee.ac.uk), Lluís Nieto MD (lnietofernandez@gmail.com)⁴,
7 Andrew Brown PhD (a.z.t.brown@dundee.ac.uk)⁶, José Román Escudero MD
8 (jescuderor@santpau.cat)^{1,2}, Ana Viñuela PhD# (ana.vinuela@newcastle.ac.uk)⁷, Mercedes
9 Camacho PhD# (mcamacho@santpau.cat)¹, Maria Sabater-Lleal PhD#
10 (msabater@santpau.cat)^{1,8,9}

11

12 #These authors equally contributed as senior authors.

13

14 Affiliations:

15

- 16 1. Unit of genomics of Complex Diseases, Institut de Recerca Sant Pau (IR SANT PAU), Sant Quintí 77-79,
17 08041 Barcelona, Spain
18 2. Servei d'Angiologia i Cirurgia Vasculard i Endovascular, Hospital de la Santa Creu i Sant Pau, Sant Antoni
19 Maria Claret 167, 08025 Barcelona, Spain
20 3. Centro de Investigación Biomédica en Red de Enfermedades Cardiovasculares (CIBERECV), Madrid,
21 Spain
22 4. Department of Vascular and Endovascular Surgery, Hospital del Mar, Passeig Marítim 25-29, 08003,
23 Barcelona, Spain
24 5. Department of Medicine and Surgery, Universitat Pompeu Fabra, Barcelona, Spain
25 6. Population Health and Genomics, Ninewells Hospital and Medical School, University of Dundee,
26 Dundee, DD1 9SY, United Kingdom.
27 7. Biosciences Institute, Faculty of Medical Sciences, University of Newcastle, Newcastle upon Tyne, NE1
28 4EP, United Kingdom
29 8. Cardiovascular Medicine Unit, Department of Medicine, Karolinska Institutet, Stockholm, Sweden
30 9. Centro de Investigación Biomédica en Red de Enfermedades Raras (CIBERER), Madrid, Spain

31

32

33 Corresponding author:

34

35 Maria Sabater-Lleal, PhD
36 Genomics of Complex Disease Unit, Institut de Recerca Sant Pau (IR SANT PAU)
37 St Quintí 77-79, 08041, Barcelona, Spain
38 Phone +34932919000; Email: msabater@santpau.cat

39

40 **ABSTRACT**

41 Background:

42 Abdominal aortic aneurysms (AAA) are focal dilatations of the abdominal aorta. They are
43 normally asymptomatic and progressively expand, increasing their risk of rupture. Rupture of
44 an AAA is associated with high mortality rates, but the mechanisms underlying the initiation,
45 expansion and rupture of AAA are not yet fully understood. This study aims to characterize and
46 identify new genes associated with the pathophysiology of AAA through differential expression
47 analyses between dilated and non-dilated aortic tissue samples, and between AAA of different
48 diameters. Our study used RNA-seq data on 140 samples, becoming the largest RNA-seq
49 dataset for differential expression studies of AAA.

50 Results:

51 We identified 7,454 differentially expressed genes (DEGs) between AAA and controls, 2,851 of
52 which were new compared to previous microarray studies. Notably, a novel cluster on
53 adenosine triphosphate synthesis regulation emerged as strongly associated with AAA.
54 Additionally, exploring AAA of different diameters identified eight genes (*EXTL3*, *ZFR*, *DUSP8*,
55 *DISP1*, *USP33*, *VPS37C*, *ZNF784*, *RFX1*) that overlapped with the DEGs between AAA and
56 controls, implying roles in both disease onset and progression. Seven genes (*SPP1*, *FHL1*, *GNAS*,
57 *MORF4L2*, *HMG1*, *ARL1*, *RNASE4*) with differential splicing patterns were also DEGs between
58 AAA and controls, suggesting that splicing differences contribute to the observed expression
59 changes and the disease development.

60 Conclusions:

61 This study identified new genes and pathways associated with AAA onset and progression and
62 validated previous relevant roles of inflammation and intracellular calcium regulation. These

63 findings provide insights into the complex mechanisms underlying AAA and indicate potential
64 targets to limit AAA progression and mortality risk.

65 **KEYWORDS:** Abdominal aortic aneurysm, RNAseq, transcriptomics, differential expression,
66 ischemic time, alternative splicing, allelic specific expression.

67

68

69

70

71

72

73

74

75

76

77

78

79

80

81

82

83

84 **BACKGROUND:**

85 Abdominal aortic aneurysms (AAA) are characterized by a local dilation of the infrarenal
86 abdominal aorta to about 1.5 times the normal adjacent aortic diameter or more than 3 cm in
87 maximum diameter[1]. AAA is accompanied by chronic inflammation, apoptosis of vascular
88 smooth muscle cells and neovascularization[2,3]. Additionally, extracellular matrix degradation,
89 microcalcification, and oxidative stress contribute to the degeneration of the aorta[1,2]. The
90 disease is progressive, and most aneurysms develop without causing symptoms[1]. However, in
91 the event of AAA rupture, mortality rates can reach 80 %[4]. The only effective treatment
92 currently available for AAA is aortic tissue repair, either through open surgery or endovascular
93 repair[1,5].

94 Some risk factors are known for developing AAA, including age, male sex, smoking, and family
95 history of AAA[1]. Smoking, in addition, is also known to increase the risk of rupture[6].
96 Additionally, recent genomic studies have revealed 121 loci associated with risk of developing
97 AAA, contributing to the knowledge of the possible pathways leading to this disease[7].
98 However, there is still an insufficient understanding of the clear mechanisms that underlie the
99 initiation, propagation, and rupture of AAA.

100 The study of gene expression, known as transcriptomics, is a valuable tool for understanding
101 human disease and revealing new therapeutic targets [8,9]. Several studies have been
102 performed to study the differentially expressed genes (DEGs) between dilated aortic tissue and
103 non-dilated control aorta using microarray technology, detecting DEGs especially associated
104 with the immune and inflammatory responses, extracellular matrix remodeling and
105 angiogenesis[10–15]. In the present study, we performed RNA sequencing (RNAseq) of the
106 complete transcriptome in 140 abdominal aortic tissue samples (96 dilated aortas and 44
107 control aortas from deceased donors) from the Triple A Barcelona Study (TABS) cohort, to
108 identify new DEGs and pathways associated with the pathophysiology of AAA initiation and

109 progression, allowing for a more comprehensive analysis of the transcriptome and becoming
 110 the largest RNAseq dataset for AAA tissue. Additionally, we aimed to investigate the differences
 111 in alternative splicing patterns in the context of AAA, and the role of genetic variants in gene
 112 expression in AAA tissue. The study design is described in **Figure 1**.

113 **RESULTS:**

114 Participants characteristics:

115 **Table 1** shows the participants demographic and clinical data. Aortic tissue samples from 96
 116 AAA patients and 44 controls from the TABS cohort were used for RNAseq analysis.

Table 1: Characteristics of study participants

	Controls (N = 44)	AAA (N = 96)	P-value	Missing values (%)
Age (Years)	61.66 (21-82)	70.38 (53-87)	0.0006	0 (0)
Sex (Male)	21 (47.73)	92 (95.83)	1.00E-10	0 (0)
Smoking (Current)	8 (21.62)	27 (32.14)	0.3378	19 (13.57)
Smoking (Past)	3 (8.11)	42 (50)	2.81E-05	19 (13.57)
Aortic Diameter (mm)	NA	65.57 (38-100.12)	-	0 (0)
Hypertension (Yes)	15 (40.54)	54 (64.29)	0.0256	19 (13.57)
Dyslipidemia (Yes)	10 (27.03)	46 (54.76)	0.0087	19 (13.57)
Diabetes mellitus (Yes)	5 (13.51)	12 (14.29)	1	19 (13.57)
Peripheral arterial disease (Yes)	NA	23 (27.71)	-	57 (59.38)
Other aneurysms (Yes)	NA	25 (29.76)	-	12 (12.5)
Cerebrovascular Disease (Yes)	3 (8.11)	36 (43.9)	0.0003	21 (15)
Cardiovascular Disease (Yes)	1 (3.34)	16 (19.05)	0.0846	27 (19.29)
Chronic obstructive pulmonary disease (Yes)	1 (2.7)	15 (17.86)	0.0481	19 (13.57)

Chronic kidney disease (Yes)	2 (5.4)	17 (20.24)	0.0726	19 (13.57)
-------------------------------------	---------	------------	--------	------------

Continuous variables are presented as mean (range), and categorical variables are presented as %. Two-sample t-tests and chi-squared tests were used to compare the means of continuous phenotypes and the distribution of categorical phenotypes, between AAA and control groups, respectively. Missing values were excluded from the calculations of each variable. Hypertension was defined based on clinical history and the use of antihypertensive medication. Dyslipidemia was diagnosed through clinical history and the use of hypolipidemic medication. Diabetes mellitus was identified by clinical history and the use of insulin or oral hypoglycemic medications, without differentiation between type 1 or type 2. Peripheral arterial disease was assessed based on clinical symptoms and clinical history. Other aneurysms included thoracic and visceral aortic aneurysms, iliac artery aneurysms, and popliteal artery aneurysms, and were diagnosed using computed tomography or ultrasound. Cerebrovascular diseases were determined by a history of transient ischemic attack or stroke. Cardiovascular diseases were assessed by history of acute myocardial infarction or angina pectoris, or admission with clinical symptoms, electrocardiogram changes, or a positive enzymatic curve diagnosed by a cardiologist. Chronic obstructive pulmonary disease was identified based on clinical history. Chronic kidney disease was assessed by clinical history.

117 We examined demographic and clinical variables between AAA and controls to determine
118 whether these might influence our expression levels differences. We found significant
119 differences in sex (**Additional file 1: Figure S1A**), age (**Additional file 1: Figure S1B**), smoking
120 status, and the prevalence of hypertension, dyslipidemia, cerebrovascular disease, and chronic
121 obstructive pulmonary disease between AAA patients and controls. In relation to smoking
122 status (N = 122), which is a known risk factor for AAA development and rupture, 70.3 % of
123 controls were never smokers, compared to 17.86 % of AAA patients. Among current and past
124 smokers, there were also differences, with 50 % of former smokers and 32.14 % of current
125 smokers in AAA, compared to only 8.11 % and 21.62 % respectively, in the controls (**Additional**

126 **file 1: Figure S3C**). We adjusted our regression analyses for age and sex, acknowledging their
127 potential influence on expression level differences.

128 Differential expression analyses between AAA and controls:

129 The analysis of differential expression between aortic samples from 96 AAA patients and 44
130 controls revealed 7,454 genes displaying significant differences in expression (adjusted p-value
131 < 0.05) (**Additional file 1: Figure S2A and Additional file 2: Table S1**). This number exceeds by
132 26.57 % the previous DEGs identified in comparable analyses using microarray
133 technologies[10–15]. Using GO and KEGG enrichment analyses, we found a total of 1,152 and
134 89 enriched terms, respectively (**Additional file 1: Figure S3A and Figure S4A**). The complete
135 results of the enriched terms for GO and KEGG are shown in **Additional files 3 and 4: Tables S2**
136 **and S3**. To better characterize the biological processes associated with the DEGs in the
137 enrichment analysis, we performed a cluster analysis of GO pathways. We found that most of
138 the DEGs were associated with the immune system: regulation of mononuclear cell
139 proliferation, leukocyte chemotaxis, regulation of adaptive immune response based on somatic
140 recombination of immune receptors built from immunoglobulin superfamily domains, mast cell
141 degranulation, major histocompatibility complex (MHC) class II protein complex, positive
142 regulation of T cell activation, and CD4-positive alpha-beta T cell differentiation (**Figure 2A**).
143 Other represented metabolic pathways were related to sequestering of calcium ion, regulation
144 of actin filament length and adenosine triphosphate (ATP) synthesis coupled electron transport
145 (**Figure 2A**). While these analyses corroborated previous associations with inflammatory, actin
146 filament regulation and intracellular calcium regulation processes, the ATP synthesis regulation
147 pathway was a new differential expressed pathway in AAA tissue.

148 Control aortic samples from deceased organ donors have been used by us and others [10–
149 13,15]. To account for differences in gene expression between AAA and control tissue that
150 could be attributed to ischemic time (time between the donor's death and sample collection

151 when blood flow is interrupted), we removed 10,737 DEGs associated to ischemic time in the
152 GTEx aorta samples (N = 387)[16] from the total DEGs found between AAA and controls,
153 leaving 3,002 DEGs (**Additional file 1: Figure S2B and Additional file 5: Table S4**).

154 We then performed a new enrichment analysis and identified 424 enriched GO terms and 65
155 KEGG pathways (**Additional file 1: Figure S3B and Figure S4B**) (Complete results are available
156 at **Additional files 6 and 7: Tables S5 and S6**, respectively), which represented removal of 728
157 and 24 pathways susceptible of being caused by ischemic time, respectively. Cluster analysis of
158 GO enriched terms confirmed identified clusters related to the regulation of calcium ion
159 retention, ATP synthesis coupled electron transport, and immune response centered on T cell
160 activation (MHC class II protein complex, positive regulation of T cell activation). On the other
161 hand, other clusters also associated with the immune system were no longer represented
162 (regulation of mononuclear cell proliferation, leukocyte chemotaxis regulation of adaptive
163 immune response based on somatic recombination of immune receptors built from
164 immunoglobulin superfamily domains, CD4-positive, alpha-beta T cell differentiation, mast cell
165 degranulation) together with the regulation of actin filament length (**Figure 2B**). By accounting
166 for genes whose expression was altered by ischemic time, we identified a set of genes that are
167 less likely to be affected by the experimental limitations of these types of studies.

168 Vascular inflammation has been previously associated to AAA development and
169 progression[17,18]. Even in our most stringent analysis, which removed pathways possibly
170 caused by ischemic time, there was a notable enrichment of pathways associated with the
171 immune response. Consequently, we decided to investigate the influence of the inflammatory
172 infiltrate on AAA by comparing the abundance of 22 immune cell types from gene expression
173 profiles between our AAA and control samples. After correcting for multiple testing, we found
174 significant differences on the abundances of CD8 T-cells, natural killer (NK) resting cells, and
175 dendritic activated cells (**Figure 2C**). AAA samples had a higher proportion of CD8 T-cells, while

176 controls had more NK resting cells and dendritic activated cells. **Table 2** provides a summary of
 177 the three cell populations with the highest and lowest presence in each group. The findings
 178 support the previously reported involvement of CD8 T-cells and NK cells in AAA.[17,18] The
 179 lower levels of dendritic cells detected in AAA were unexpected, as previous studies found
 180 significantly higher levels of dendritic cells in AAA samples compared to controls[19].

181 **Table 2: Summary of the three most and least prevalent cell populations in AAA and controls.**

Cell Populations (AAA)	Percentage (%)	Cell Populations (Controls)	Percentage (%)
Plasma B cells	9.46	Resting mast cells	12.34
M2 macrophages	8.68	Resting memory CD4 T cells	8.31
Resting mast cells	6.99	M2 Macrophages	8.23
M1 macrophages	1.43	Eosinophils	2.03
Eosinophils	1.37	T cell follicular helper cells	1.94
Activated dendritic cells	1.13	M1 Macrophages	1.45

182

183 Study of alternative splicing:

184 The relevance of alternative splicing in the development of diseases, such as cancer,
 185 neurological, and cardiovascular diseases has been well-established for years.[20] However,
 186 capturing the complexity of alternative splicing has been challenging. With the recent
 187 improvements in sequencing techniques it is now possible to study alternative splicing in more
 188 depth.[20] We investigated alternative splicing patterns between the AAA and control groups
 189 to identify specific splicing patterns associated with AAA. We identified 15 significant
 190 alternative splicing events on eleven unique genes (*FHL1, GNAS, ASAH1, SPP1, ARL1, MORF4L2,*
 191 *CYCS, HMGB1, HMG1, SELENOP, RNASE4*) between AAA and controls. The analysis revealed
 192 that, as anticipated, the number of altered alternative first exon events was more represented
 193 than any other splice event among AAA and control samples (**Figure 3A**), consistent with

194 previous work suggesting that it is the most frequent splice event in the human genome[21]
195 (Complete results are available in **Additional file 8: Table S7**). A functional enrichment analysis
196 was conducted on the eleven genes with significant alternative splicing events, but no
197 significantly enriched metabolic pathways were found. Interestingly, seven out of the eleven
198 genes were also differentially expressed between AAA and controls, suggesting that the
199 expression of specific splicing variants could be altered in AAA (**Figure 3B**).

200 Differential expression analysis by aortic diameter:

201 The diameter of AAA is a significant risk factor for rupture. We analyzed the DEGs by diameter
202 to identify alterations in gene expression throughout the progression of the disease. We
203 observed a total of 32 DEGs among aneurysms of varying diameters (N = 84), although no
204 enriched pathways were identified (**Additional file 1: Figure S2C and Additional file 9: Table**
205 **S8**). Of the 32 DEGs by diameter, eight were also DEGs between AAA and controls (**Figure 3C**),
206 suggesting that these eight genes are relevant for disease formation and also during disease
207 progression.

208 Allelic specific expression:

209 We investigated the potential effect of AAA-associated genetic variants on gene expression in
210 diseased tissue by studying allele specific expression in twelve AAA samples with available
211 genetic data. On average, we identified 529 genes with significant allele specific expression
212 (adjusted p-value < 0.05) in the twelve AAA samples. Among these genes, 90 exhibited
213 significant allele specific expression in more than five of the twelve AAA samples. Additionally,
214 to determine whether these associations were related to AAA or were characteristic of the
215 aortic tissue, we compared allele specific expression patterns between our AAA samples and
216 387 GTEx aortic samples, used as controls. The comparison between AAA and control samples
217 identified 1,815 genes with significant differences in the allele specific expression patterns
218 (adjusted p-value < 0.05) (**Figure 4A**). An enrichment analysis on GO terms for these 1,815

219 genes revealed 91 enriched pathways. The posterior cluster analysis revealed three clusters
220 strongly related to the immune system: MHC protein complex, positive regulation of T cell-
221 mediated cytotoxicity, and regulation of T cell activation (**Figure 4B**). The association between
222 the immune system and AAA was also observed in the differential expression analysis between
223 AAA samples and controls, validating the robustness of these results.

224 Finally, among the 90 genes that exhibited significant allele specific expression in more than
225 five AAA samples, we selected those that also showed significant differential allelic specific
226 expression analysis between AAA and GTEx control samples, and those present in loci
227 identified in the largest genome-wide association study (GWAS) on AAA risk[7], in order to
228 identify haplotypes associated with AAA risk. Among the selected genes, *SNURF* was the only
229 gene that also presented differential allele specific expression patterns between AAA and
230 control tissues, and *SPP1* and *THBS2* were prioritized based on their presence in a locus
231 identified in the previous GWAS on AAA. This allowed to hypothesize that the presence of
232 particular genetic haplotypes in these three genes determined their differential expression
233 associated with risk of AAA.

234 **DISCUSSION:**

235 This study analyzes differential expression between AAA aortic tissue samples and control
236 aortic samples using whole transcriptome data obtained through RNAseq. In addition, we
237 studied the effect of ischemic time on gene expression, to obtain a more credible list of genes
238 associated with AAA development. Using our RNAseq data, which provides superior alternative
239 splicing analysis compared to microarrays[22], we conducted a novel exploration of alternative
240 splicing between AAA and control samples, to identify potential causes of the observed
241 differential expression. Furthermore, we analyzed the differential expression between AAA of
242 different diameters to study the genes altered during disease progression. Finally, we analyzed

243 allele specific expression to gain insights into how genetic variants impact expression in the
244 diseased tissue.

245 Study of ischemic time-independent pathways involved in AAA development:

246 Clustering analysis with the enriched pathways after accounting for the ischemic time effect
247 revealed a strong association with MHC class II protein complex, positive regulation of T-cells,
248 and intracellular calcium ion regulation. Additionally, we have for the first time identified the
249 regulation of the ATP synthesis pathway in a differential expression analysis of aortic samples.
250 While the detection of the ATP synthesis regulatory pathway is novel, it is in line with previous
251 work associating mitochondrial dysfunction and AAA [23,24]. On the other hand, previous
252 differential expression studies in microarrays between AAA and control aortic tissue have
253 consistently found associations of immune system pathways with AAA.[10–13,15] Our results
254 confirm these associations and demonstrate that these are independent of the ischemic time,
255 which is a confounder factor in most studies using donor samples. Finally, the regulation of
256 intracellular calcium was previously detected in one study of differential expression between
257 dilated and non-dilated aortic samples[11]. Our analyses confirm that this association is
258 independent of ischemic time.

259 We identified for the first time several enriched signaling pathways, with a large presence of
260 genes that code for subunits of complexes I (NADH ubiquinone oxidoreductase), III (Ubiquinol-
261 cytochrome c reductase) and IV (cytochrome c oxidase)) of the electron transport chain. Our
262 results indicate that 88 % (22 / 25) of the DEGs coding for the subunits of the complexes that
263 form the electron transport chain are expressed to a lower extent in AAA, suggesting a lower
264 synthesis of ATP in AAA tissue. Mitochondrial dysfunction has previously been studied in the
265 development of AAA[23,24] and other cardiovascular diseases[25] due to its key role in some
266 of the cellular alterations characteristic of cardiovascular diseases, including excessive
267 production of reactive oxygen species, energy depletion, endoplasmic reticulum stress, and

268 activation of apoptosis. However, this is the first time that these metabolic pathways have been
269 characterized in a DEGs study of AAA, confirming the role of mitochondrial dysfunction on AAA.

270 Among the genes present in all the enriched signaling pathways related to intracellular calcium
271 regulation, *APLNR*[26], *F2R*[27], *GPER1*[19], *JPH2*[28], *PKD2*[29] and *THY1/CD90*[30] have
272 already been investigated for their role in AAA. However, six additional genes are present in all
273 pathways: *ABL1*, *CALM1*, *CALM2*, *RYR2*, *SRI* and *CD19*. Except for *CALM2*, all of them have been
274 previously identified as DEGs in previous microarray studies between AAA and control
275 samples[10–12,15], but none of these genes have been further investigated in either functional
276 or epidemiological studies. These genes are closely related to intracellular calcium metabolism.

277 *ABL1* participates in both the release of stored intracellular calcium and extracellular calcium
278 entry[31]. *CALM1* and *CALM2* code for two isoforms of the calmodulin protein, which plays a
279 crucial role in the contraction of vascular and cardiac tissue through the detection of
280 intracellular calcium[32]. *RYR2* is mainly expressed in cardiac tissue and codes for the main
281 regulator of sarcoplasmic calcium release[33]. *SRI* codes for the main binding protein of the
282 *RYR2* gene product[34]. The comparison between our AAA and control samples shows a
283 downregulation of all these genes, suggesting a decrease in intracellular calcium levels in
284 smooth muscle cells, consistent with loss of vascular contractility in the dilated aorta[35].

285 On the other hand, we observed upregulation of the *CD19* gene in AAA. The activation of the
286 surface protein encoded by *CD19* triggers the release of intracellular calcium, which contrasts
287 with the previous results[36]. However, *CD19* is also a biomarker of B-cell development [36]
288 which also play a key role in the development of AAA[37].

289 Among the pathways that were previously identified in differential expression analyses
290 between AAA and control tissue is inflammation. There is a widely studied inflammatory
291 component in AAA development involving both, adaptative and innate immune responses
292 [17,18]. The presence of inflammatory infiltrates in AAA tissue have been widely

293 demonstrated, which play a key role in the development of the disease[17,18]. The results of
294 our cluster analysis also corroborated the association with the immune system after accounting
295 for ischemic time, highlighting the key role of T cells on AAA development[38,39].

296 To better understand the effects of the inflammatory infiltrate in AAA development, we
297 compared the proportions of inflammatory infiltrates between AAA and control samples. Some
298 previous studies have analyzed the inflammatory infiltrates in AAA tissue[15,19,40]. In one
299 study[15], immune cell proportions were estimated in AAA tissue layers (media and adventitia),
300 without comparing with controls. Our results strongly corroborate their findings, suggesting
301 that plasma B cells and M2 macrophages were the two most represented cell populations in
302 both layers, and M1 macrophages, eosinophils, and activated dendritic cells were among the
303 least represented cells in both layers. Surprisingly, resting mast cells emerged as our third most
304 represented cell group, while in the layer-specific analysis, mast cells represented a small
305 percentage of the total inflammatory cells. This contrasts with another study that compared
306 whole-tissue samples between AAA and controls[19], where resting mast cells were among the
307 most frequent cell groups in AAA samples. In addition, our results align with this study in
308 detecting higher proportions of CD8 T-cells and lower proportions of resting NK cells in AAA
309 samples. However, a discrepancy was noted in the levels of activated dendritic cells, which
310 were more present in controls in our study but slightly higher in AAA samples in the previous
311 work. Additional single-cell data demonstrated a higher proportion of T follicular helper cells
312 and lower proportions of M1 and M2 macrophages in AAA samples compared to controls[40].

313 To rule out the effect of death as potential cause of variability, we used a reference work that
314 evaluated the effect of death in blood samples,[41] which found higher levels of resting NK
315 cells and CD8 T-cells in post-mortem samples. These results suggest that the increase in CD8 T-
316 cells levels in AAA tissue could be even greater than the one we observed, and that the greater
317 presence of NK resting cells in control samples could be due, in part, to their origin from organ

318 donors. Consistent with this hypothesis, previous studies have shown that levels of NK cells are
319 higher in the peripheral blood of AAA patients compared to controls,[42] and that these cells
320 play a role in the development of the disease[18]. These results also suggest the existence of a
321 highly cytotoxic environment led by CD8 T-cells in AAA tissue.

322 The lower levels of activated dendritic cells in the AAA samples compared to the controls was
323 unexpected, given their established role as AAA inducers[17,19]. These results suggest that,
324 although dendritic cells may participate in the development of AAA, they are not part of the
325 inflammatory infiltrate.

326 Study of alternative splicing between AAA and controls:

327 This is the first study to elucidate the role of splicing in AAA development. We compared splice
328 events between AAA and controls and identified eleven genes (*SPP1*, *FHL1*, *GNAS*, *MORF4L2*,
329 *HMGN1*, *ARL1*, *RNASE4*, *ASAH1*, *CYCS*, *HMGB1*, *SELENOP*) with differentially represented
330 splicing variants. We compared the splice events types identified in our comparison between
331 AAA and controls samples with the presence of splicing events in the whole genome [21] and
332 the observed proportions were comparable to the expected values genome-wide. The most
333 frequent splicing types were alternative first exon (60 %) and skipping exon (20 %), while the
334 least frequent were alternative 5' splice-site (13.3 %) and mutually exclusive exon (6.67 %). On
335 the other hand, it was surprising that our results did not include alternative last exon,
336 alternative 3' splice-site, and retained intron, despite their considerable genome-wide
337 frequencies (10.72 %, 9.2 % and 3.54 %, respectively). This may be due to the limited sample
338 size, as only 15 events were identified.

339 We observed seven genes that showed differential expression between AAA and control
340 samples and had a splicing variant significantly more represented in AAA or controls (*SPP1*,
341 *FHL1*, *GNAS*, *MORF4L2*, *HMGN1*, *ARL1*, *RNASE4*), indicating that splicing differences could be
342 explaining the observed differential expression. Among these genes, *SPP1* and *FHL1* have been

343 previously characterized in relation to AAA[43,44], whereas *GNAS* is a new DEG identified
344 between AAA and control tissue. The evidence of differential splicing events validates *GNAS* as
345 a new robust DEG between AAA and control tissue, and suggests that alternative splicing in this
346 gene explains the differential expression and its implication to AAA. Finally, *MORF4L2*, *HMG1*,
347 *ARL1* and *RNASE4* although they have been identified in previous differential expression
348 studies in relation to AAA[10–15], their specific role in AAA has not been studied. For these
349 genes, our results contribute to understand the molecular mechanism leading to differential
350 expression in AAA tissue.

351 *SPP1* codes for the osteopontin protein, an important regulator of inflammation that has
352 described functions in cardiovascular diseases[45]. *SPP1* is more expressed in AAA tissue than
353 controls, both in animal models and in humans, and it participates in AAA-associated
354 extracellular matrix degradation[46,47] through the nuclear factor kappa B signaling pathway.
355 It is also known that the *SPP1* gene undergoes splicing and gives rise to 3 distinct isoforms
356 osteopontin a, osteopontin b and osteopontin c, with specific characteristics, which have not
357 been characterized in AAA. Consistent with previous data, our results found increased
358 expression in AAA tissue, and identified for the first time that that skipping of exon 3 on *SPP1*
359 gene is more frequent in AAA than in controls, suggesting that this form of alternative splicing
360 may be important for the development of AAA.

361 *FHL1* codes for a protein that is highly expressed in skeletal and cardiac muscle. *FHL1* has been
362 shown to be a promising blood biomarker for human ascending thoracic aortic aneurysm as a
363 modulator of metalloproteases.[44] Our findings, and those obtained in previous microarray
364 studies[10–13,15], indicate that *FHL1* levels are lower in AAA than in controls. We have
365 detected for the first time that an alternative 5' splicing-site form in this gene occurs more
366 frequently in the control group, suggesting that AAA tissue would have reduced expression of
367 this alternative isoform and reduced levels of *FHL1*, leading to higher risk of AAA development.

368 Although not previously found in transcriptomic studies, mutations in the *GNAS* gene have
369 been studied in mice for their effect promoting AAA[48]. *GNAS* codes for the alpha subunit of
370 the heterotrimeric G stimulatory protein ($G\alpha$). $G\alpha$ may play a protective role in AAA
371 development through regulation of vascular muscle tissue and is considered a potential
372 therapeutic target[48]. Consistent with this protective role, our results confirmed lower
373 expression *GNAS* levels in AAA. Moreover, our results add a mechanistic insight by revealing an
374 alternative first exon splicing variant that occurs more frequently in controls and that could
375 increase expression levels of the final protein and protect against AAA.

376 *MORF4L2* and *HMG1* are DNA repair related genes, which had significantly lower and higher
377 expression levels in AAA tissue compared to control tissue, respectively. *MORF4L2* has been
378 associated with atheroma plaque progression in atherosclerosis[49]. Both genes present
379 alternative splicing events that are less frequent in AAA tissue. Further work to elucidate the
380 specific role of these genes in the risk of AAA development is warranted.

381 Genes associated with AAA onset and progression:

382 We identified eight genes (*EXTL3*, *ZFR*, *DUSP8*, *DISP1*, *USP33*, *VPS37C*, *ZNF784*, *RFX1*) that
383 showed differential expression between AAA and control tissues, and also differential
384 expression in AAA tissues of different diameters. Among these, *EXTL3*, *ZFR*, *DUSP8*, and *DISP1*
385 have been previously identified as DEGs between AAA and controls but their role in AAA
386 progression is novel.[10–15], and *USP33*, *VPS37C*, *ZNF784* and *RFX1* are novel DEGs. This could
387 indicate that the genes may have a role beyond the disease onset and could be potential
388 therapeutic targets to halt aneurysm expansion. Therefore, the potential contribution of these
389 genes to the development of AAA needs to be thoroughly investigated.

390 Among the genes with higher expression at larger diameters, *USP33* encodes a
391 deubiquitinating enzyme that has been associated with the development of hypertension[50],
392 a known risk factor for AAA[51]. Proteins with deubiquitinating functions have been proposed

393 as possible candidate genes for the treatment of AAA and other cardiovascular diseases[52].
394 Additionally, *USP33* promotes the stabilization of beta2-adrenergic receptors, which promote
395 vasodilation in smooth muscle[53]. We observed an increase in *USP33* expression with
396 increased AAA diameter, which is consistent with the functionality of beta2-adrenergic
397 receptors. These results suggest that the *USP33* gene may be a potential candidate for the
398 treatment of AAA.

399 Among the genes that exhibit lower expression levels with larger diameters, we highlight
400 *DUSP8* and *RFX1*. *DUSP8* is a phosphatase that negatively regulates the MAP kinase pathway,
401 which is linked to cell differentiation and proliferation[54]. Previous studies have shown that
402 *DUSP8* expression levels are downregulated in mouse models of aortic dilatation[55], and the
403 dual specificity phosphatase 8 protein (*DUSP8*) acts as a regulator of cardiac dynamics[54]. Our
404 findings align with those obtained in the animal model of aortic dilatation, suggesting that
405 *DUSP8* may be a potential candidate gene for treating AAA by regulating both aortic dilatation
406 and the immune system. *RFX1* encodes a transcription factor that regulates genes involved in
407 MHC class II[56]. In a previous bioinformatics study using microarray data, *RFX1* was identified
408 as a transcription factor that could potentially regulate DEGs between AAA and controls
409 through its downregulation[57]. Previous research has shown that a decrease in *RFX1*
410 expression leads to activation of CD14⁺ monocytes in CAD patients[58]. Furthermore, CD14
411 protein plays a crucial role in recruiting macrophages during the early stages of AAA, and
412 knockout mice for *CD14* gene have been shown to resist the formation of AAA in two different
413 models[59]. Finally, our expression results indicate that *CD14* is upregulated in AAA patients
414 compared to controls (FDR P-value = 0.002). In conclusion, these results suggest that low
415 expression levels of the transcription factor *RFX1* may lead increased *CD14* expression, which
416 plays a crucial role in the development and progression of AAA by recruiting macrophages.

417 Two previous studies have considered the diameter of AAA in differential expression analyses
418 with aortic tissues. The first study[10] compared gene expression between small (n = 20) and
419 large AAA (n = 29) with controls, but did not compare AAA of varying diameters. The second
420 study[15] performed a correlation analysis on each gene between the diameter growth rate
421 and gene expression in individuals (n = 24) with two aortic measurements, distinguishing
422 between the media and adventitia aortic layers but did not identify any significant genes after
423 multiple testing correction. The larger sample size in our study have enabled to identify for the
424 first time genes that are associated to aneurysm progression, which could be potential
425 therapeutic targets.

426 Identification of haplotypes associated with AAA risk:

427 We performed a clustering analysis of enriched biological pathways with the 1,815 genes with
428 significant differences in the allele specific expression patterns between AAA and controls. The
429 cluster analysis revealed a strong association with immune system pathways, particularly those
430 associated with T cells. These results are consistent with the clustering analysis of DEGs
431 between AAA and controls and demonstrate how specific haplotypes determine the
432 differential expression of genes associated with AAA in the diseased tissue. By combining allele
433 specific expression information on AAA samples with the allelic specific expression results
434 between AAA and controls, along with information from a previously published GWAS[7], we
435 explored the associations between genetic variants associated with AAA risk and gene
436 expression. This approach aimed to unravel the association between genetic haplotypes and
437 gene expression as determinants of AAA risk.

438 *SNURF* is the only gene that showed significant allelic specific expression in more than five of
439 the twelve studied individuals with AAA and differential allelic specific expression patterns
440 between AAA and controls suggesting the existence of a specific haplotype associated with less
441 expression in AAA and leading to higher risk of AAA. *SNURF* codes for an open reading frame of

442 the *SNRPN* gene, with which it forms a bicistronic gene[60]. Both genes exhibit significantly
443 lower expression in AAA than in controls in our data. Moreover, we observed that rs705 single
444 nucleotide polymorphism (SNP) (minor allele frequency (MAF) (C) = 0.45) determined *SNURF*
445 expression in eight out of twelve AAA samples, where the T allele was associated with double
446 expression amounts compared to the C allele. Additionally, rs705 is an eQTL in blood of the
447 *SNRPN* gene. Although causality cannot be derived from these results, these results suggest a
448 possible effect of the haplotype containing the rs705 T allele on this locus on *SNURF*
449 expression, resulting in higher risk for AAA development.

450 Among the genes with significant allele specific expression in the twelve analyzed AAA samples
451 that did not exhibit significant allele specific expression patterns between AAA and control
452 groups in our analyses, we selected those that were part of a locus associated to AAA in the
453 most recent GWAS on AAA risk[7]. *THBS2* encodes for thrombospondin 2, a protein that
454 regulates cell-cell and cell-extracellular matrix interactions and has been studied in relation to
455 multiple cardiovascular diseases[61]. *THBS1*, a member of the same family, has been identified
456 as a regulator of AAA in animal models[62]. Our allele specific expression results suggest that
457 the expression of this gene could be associated with AAA development, supporting the
458 implication of the gene in AAA risk. Two common genetic variants (rs58023137 (MAF (T) = 0.22)
459 and rs9505895 (MAF (A) = 0.2)) were identified in previous GWAS studies[7] and in our allele
460 specific expression results. For both variants, the GWAS risk allele was associated with higher
461 expression gene levels in one individual with AAA. Additionally, these two variants were also
462 eQTLs in aortic tissue regulating *THBS2* gene expression, confirming the known association
463 between thrombospondin and AAA[7], and demonstrating the presence of risk haplotypes
464 associated to increased expression and risk of AAA.

465 Regarding the *SPP1* gene, we found six genetic variants (rs35893069 (MAF (T) = 0.1), rs6839524
466 (MAF (G) = 0.12), rs4754 (MAF (C) = 0.28), rs1126616 (MAF (T) = 0.27), rs1126772 (MAF (G) =

467 0.21), rs9138 (MAF (C) = 0.22)) with allele specific expression among the twelve AAA samples.
468 As previously discussed, the *SPP1* has been associated to AAA risk due to the role of the
469 protein osteopontin, which it encodes, in the degradation of the extracellular matrix that is
470 characteristic of AAA[46,47]. However, none of the six genetic variants were found to be
471 significant in the previous GWAS[7], and therefore no association with allelic expression could
472 be established.

473 Strengths and limitations and comparison with previous studies

474 This is one of the largest studies of differential expression between AAA tissue samples and
475 controls. However, due to the difficulty in obtaining aortic tissue samples, the sample size is
476 still limited compared to transcriptomic studies in more accessible tissues, which may have
477 limited our power. Previous studies comparing transcriptomics between AAA and control
478 samples have been limited to the use of expression microarrays[10–15]. In this study, we used
479 RNAseq to obtain transcriptomic information. RNAseq provides greater sensitivity, a wider
480 range of detection of both high and low expression genes, and is not limited to microarray
481 probes[9,63], which allowed us to detect more DEGs. Additionally, RNAseq technology allowed
482 for a more precise study of alternative splicing compared to microarrays.

483 Accounting for ischemic time enabled us to more accurately identify biological processes
484 associated to AAA, thereby minimizing differences in sample origins between AAA and
485 controls. At the same time, despite ensuring more robust findings, the elimination of these
486 genes could have been too rigorous and imply the loss of some biological pathways associated
487 with AAA that, at the same time were affected by ischemic time.

488 The significant phenotypic differences in age and sex between individuals recruited as AAA and
489 controls are a limitation of the study. Moreover, the analyses of the allele specific expression
490 are limited by the small sample size (n = 12) and the requirement for the individuals to be
491 heterozygous in order to study the genetic variants. Therefore, further validation is necessary.

492 However, this is the first study analyzing allele specific expression in AAA and our results
493 emphasize the value of this new dataset combining genetic and expression data for the study
494 of AAA.

495 Finally, the conclusions presented in this article are based on the results obtained from a
496 cohort of European- ancestry individuals only. Further analyses in different ancestries will
497 determine the generalization of these results.

498 **CONCLUSIONS**

499 Our analysis of the whole transcriptome has enabled us to identify numerous novel genes that
500 were not previously detected in microarray studies. Additionally, our efforts to account for the
501 impact of ischemic time have provided more robust implicated biological pathways that lead to
502 AAA development. Among these pathways, ATP synthesis regulation (i.e. genes encoding
503 subunits I, III and IV of the electron transport chain), has been associated for the first time in
504 transcriptomic studies of AAA tissue, although this pathway was previously studied in relation
505 to AAA in previous studies[23,24]. Additionally, the study of differential splicing processes
506 between AAA and controls have revealed novel molecular processes involving already known
507 genes in relation to AAA, such as *SPP1*, *FHL1* or *GNAS*.

508 The study also analyzed the differential expression of genes in individuals with AAA of different
509 diameters, providing valuable insights into the underlying molecular mechanisms contributing
510 to AAA progression. Further research on these genes may lead to potential treatments against
511 aneurysm expansion, which increases the risk of rupture. Finally, the analysis of differential
512 allele specific expression in twelve AAA has allowed the identification of haplotypes associated
513 with expression of certain genes and AAA risk, providing evidence for their involvement in
514 disease, and shedding light into the molecular mechanism.

515 Overall, this study provides a comprehensive exploration of AAA expression patterns, revealing
516 key insights into the pathophysiology of AAA initiation and progression. RNAseq was used to

517 conduct one of the largest differential expression analyses to date, uncovering numerous genes
518 associated with AAA. Our consideration of ischemic time and AAA diameter improved the
519 precision in identifying biological processes associated with AAA onset and progression.
520 Furthermore, our analysis of differential allele specific expression has identified genetic
521 haplotypes that influence gene expression on AAA tissue, which advances our understanding of
522 AAA genetic background. These findings contribute to future research and potential advances
523 in precision medicine to reduce AAA progression and mortality risk.

524 **METHODS:**

525 Subjects:

526 We used a total of 140 human abdominal aortic samples from 96 patients diagnosed with
527 infrarenal AAA and undergoing open surgery for AAA repair at *Hospital de la Santa Creu i Sant*
528 *Pau* and *Hospital del Mar* (Barcelona) and 44 controls. The study participants were obtained
529 from TABS cohort, which includes genomic, transcriptomic, clinical, and maximum aneurysm
530 size data, from AAA patients and healthy individuals. Maximum aortic diameters were obtained
531 from computed tomography or ultrasound images. Genomic data were obtained through
532 genotyping using the Infinium Global Screening Array-24 v2.0 from Illumina (San Diego,
533 California) (coverage 665,608 variants) and imputation to the TOPMED Reference Panel. Only
534 variants with imputation quality > 0.3 were used for the allele specific expression analyses.
535 Healthy abdominal aortas were obtained from 21 male and 23 female multiorgan donors
536 (**Table 1**).

537 Sample processing:

538 A portion of tissue sample was placed in RNeasy lysis solution (Qiagen GmbH, Hilden, Germany)
539 and stored for 24 hours at 4 °C before long-term storage at -80 °C until further processing. For
540 RNA isolation, tissues were then homogenized in 1 ml Trizol (Ambion, Carlsbad, CA) in the
541 FastPrep-24 homogenizer and Lysing Matrix D tubes (MP Biomedicals, Solon, OH) and RNA was

542 purified using PureLink RNA Mini Kit (Invitrogen, Carlsberg) following the manufacturer's
543 recommendations. RNA concentration was measured using Nanodrop 200 (Thermo Scientific).

544 RNA integrity was assessed on Agilent 2100 Bioanalyzer (Agilent, Santa Clara, CA, USA). RNA
545 integrity number (RIN) was recorded and only samples with a RIN higher than 6 were used.

546 RNA sequencing:

547 We performed sequencing analyses using Illumina NovaSeq 6000, with a read length of 150 bp
548 and paired-end sequencing. Two sequencing runs were performed to reduce the variability of
549 the technical variables. First, AAA and control samples were randomized between sequencing
550 plates. Second, only AAA were sequenced with as little technical variability as possible. In all
551 sequencing runs, a minimum of 30 million reads were required, repeating the sequencing on a
552 new plate if this limit was not reached.

553 Alignment, quantification, and quality control:

554 We used STAR v.2.5.3a[64] to perform the alignment on the reference genome version GRCh38
555 and we then used RSEM v1.3.0[65] for gene quantification. For both analyses, we used gene
556 models from GENCODE v26 gene annotation file[66]. In total, 58,219 genes were quantified. Of
557 these, we selected protein coding genes and long non-coding RNA (lncRNA) genes that had
558 been either experimentally validated (level 1 annotation) or manually annotated (level 2
559 annotation)[66], resulting in 27,290 genes (19,777 protein-coding and 7,513 lncRNA) for
560 further analyses. Gene quantifications were expressed as Transcripts Per Million (TPMs), which
561 were obtained by normalizing for gene length first, and then for sequencing depth. This
562 ensured that the sum of all TPMs in each sample was the same, facilitating the comparison
563 between samples. All samples reached a minimum of 10 million reads aligned to the reference
564 genome with STAR (**Additional file 1: Figure S5A-5B**)[64].

565 As part of the quality control, we also checked that the reported sex of the samples matched
566 the biological sex of the sequenced data. To do this, we compared the expression levels of the
567 *XIST* gene, which regulates the X chromosome inactivation mechanism in females and has null
568 expression in males, with the expression of male exclusive genes, calculating an average
569 expression of Y chromosome genes. One sex mismatch sample was eliminated from the study
570 (**Additional file 1: Figure S5C**).

571 Differential expression analysis:

572 Before conducting differential expression analyses, we normalized the TPMs counts using
573 quantile normalization and removed lowly expressed genes by removing genes with less than
574 0.5 TPMs in more than 50% of the samples. For the comparison of AAA against control
575 samples, we kept 14,675 genes and removed 12,615 genes. For the comparisons among AAA
576 using the AAA-only sequencing panel, we kept 14,779 genes and removed 12,511 genes.

577 To evaluate the impact of technical covariates on the results, we performed a Principal
578 Components (PC) Analysis on all samples and tested the correlation between the PC Analysis
579 and all the technical covariates. Technical covariates that had significant correlations (p-value <
580 0.05) with the first four PC were included in the analyses as fixed effect covariates. Additionally,
581 all comparisons were adjusted for age and sex. To preserve the regulatory effects that act
582 through smoking, we did not include smoking as a covariate (**Additional file 10: Table S9**).

583 First, we calculated DEGs between AAA and controls using a linear regression, including age,
584 sex, flow cell type, flow cell lane, GC mean content (GC mean), RIN, percentage of RNA
585 fragments > 200 (DV200), and Qubit as covariates. Date of creation of the library was not
586 included due to its high correlation with the case/control variable (Pearson's correlation = -
587 0.74) (**Additional file 1: Figure S6A-6B**). Second, we calculated DEGs between aneurysms of
588 varying diameter using a linear regression, including age, sex, date of creation of the library,
589 batch number, GC mean, RIN, DV200 and Qubit. We corrected for multiple testing in both

590 analyses using Benjamini-Hochberg false discovery rate (FDR) method and considered
591 significant DEGs those with an adjusted p-value below 0.05[67].

592 We then performed a linear regression model to identify genes whose expression could be
593 altered by ischemic time, using ischemic time information on artery aorta tissue samples from
594 GTEx V8 data[16]. We corrected the linear regression model for age, sex, RIN, type 2 diabetes,
595 body mass index, autolysis score, center, sequencing protocol, sequencing platform, and
596 genotyping PC. To determine the genes affected by ischemic time, we corrected for multiple
597 testing and selected genes with an FDR-adjusted p-value lower than 0.05[67]. All analyses were
598 performed in R.

599 Enrichment analysis:

600 After identifying DEGs between AAA and control samples and between AAA of varying
601 diameters, we performed enrichment analyses using the R package ‘clusterprofiler’[68,69] on
602 the Gene Ontology (GO) databases for Biological Process, Cellular Component and Molecular
603 Function, as well as the Kyoto Encyclopedia of Genes and Genomes (KEGG)[70]. We corrected
604 for multiple testing using the Benjamini-Hochberg FDR method and identified significantly
605 enriched pathways with an adjusted p-value below 0.05[71]. We used ‘aPEAR’[72] to perform a
606 cluster analysis of redundant pathways with a minimum cluster of size of 15 and hierarchical
607 clustering. The enriched pathways and genes were visualized using ‘enrichplot’[73].

608 Study of the inflammatory infiltrate:

609 We investigated the differences in the proportions of inflammatory infiltrates between AAA
610 and control samples using CIBERSORTx[74]. CIBERSORTx compares RNAseq data with a
611 reference expression database of selected cell types, to estimate the proportion of each cell
612 type. The residuals of our RNA-seq data were calculated using a linear regression that included
613 all covariates except the status variable. We used the residuals and the ‘lm22’ signature matrix,
614 that contains expression data of 547 genes in 22 inflammatory cell types from microarray

615 studies, and can be used to distinguish inflammatory cell populations in RNA-seq data[74]. We
616 conducted a t-test to compare the proportions of each cell type between AAA and controls. A
617 p-value threshold corrected by multiple testing using Bonferroni for the number of cell types
618 was set at $p\text{-value} < 2.27 \times 10^{-3}$ (0.05 / 22).

619 Alternative splicing:

620 We used the SUPPA2 software to identify differences in splice events between AAA and control
621 tissue samples. SUPPA2 can identify seven different splice events including skipping exons,
622 mutually exclusive exons, alternative 5' or 3' splice sites, retained introns, and alternative first
623 or last exons. Based on gene annotation from GENCODE v26,[66] we computed the proportion
624 of splice inclusion for the TPMs counts in each splice event by dividing the number of TPMs of
625 one form of the event by the total number of TPMs. Finally, the magnitude of splicing change
626 was calculated by subtracting the proportion of splice inclusions between AAA and controls.
627 Significant alternative splicing events were selected based on a magnitude of splicing change
628 higher than 0.1 and FDR-corrected p-values lower than 0.05, using the default parameters for
629 calculation.

630 Allelic specific expression:

631 Allele specific expression was investigated using PHASER[75] on twelve AAA samples with
632 genotype data. Allele specific expression consists of the analysis of the differences in the
633 expression levels of the different haplotypes present in a heterozygous individual. We
634 quantified allele specific expression at the gene level using the GENCODE V26 gene
635 annotation[66]. To reduce the effect of the known mapping bias towards the reference
636 allele[76], we performed an additional STAR mapping step with WASP filtering[77].

637 We used the allele specific expression data obtained by the GTEx consortium to compare allele
638 specific expression between our AAA samples and GTEx control tissues[78]. To do this, we
639 compared the proportional expression of each allele between our AAA samples and the GTEx

640 controls, using a non-parametric Wilcoxon test[79]. Then, to identify genes with distinct allele
641 specific expression patterns, we corrected for multiple comparisons using FDR[67]. We
642 performed enrichment and cluster analyses in all genes showing FDR adjusted p-values lower
643 than 0.05.

644 **ABBREVIATIONS**

645 **AAA** abdominal aortic aneurysm

646 **DEGs** differentially expressed genes

647 **TABS** triple A Barcelona study

648 **LncRNA** long non-coding RNA

649 **TPMs** transcripts per million

650 **PC** principal component

651 **GC mean** GC mean content

652 **DV200** percentage of RNA fragments > 200

653 **FDR** false discovery rate

654 **GO** gene ontology

655 **KEGG** Kyoto encyclopedia of genes

656 **MHC** major histocompatibility complex

657 **GWAS** genome-wide association study

658 **ATP** adenosine triphosphate

659 **G α** heterotrimeric G stimulatory protein

660 **DUSP8** dual specificity phosphatase 8 protein

661 **SNP** single nucleotide polymorphism

662 **MAF** minor allele frequency

663 **DECLARATIONS**

664 Ethics approval and consent to participate:

665 The study was approved by the *Hospital de la Santa Creu i Sant Pau* Ethics Committee (IIBSP-
666 OMI-2019-102). All patients gave written informed consent prior to surgery to participate in
667 the study. The study conformed to the principles of the Declaration of Helsinki.

668 Consent for publication:

669 Not applicable.

670 Availability of data and materials:

671 The personal data used for this study is available from the corresponding author on reasonable
672 request for collaborations provided it complies with the ethical permits of the study. All other
673 data supporting the findings of this study is available within the paper and its Supplementary
674 Information. Code used for data preparation and analysis is available at
675 <https://github.com/Gerardts9/RNAseq>.

676 Competing interests:

677 The authors declare that they have no competing interests.

678 Funding:

679 This work was supported by a grant from the Spanish Ministry of Science and
680 Innovation (PID2019-109844RB-I00). The genotyping service was carried out at the Genotyping
681 Unit-CEGEN in the Spanish National Cancer Research Centre (CNIO), supported by Instituto de
682 Salud Carlos III (ISCIII), Ministerio de Ciencia e Innovación. CEGEN is part of the initiative

683 IMPaCT-GENÓMICA (IMP/00009) cofunded by ISCIII and the European Regional Development
684 Fund (ERDF). GT-S is supported by the Pla Estratègic de Recerca i Innovació en Salut (PERIS)
685 grant from the Catalan Department of Health for junior research personnel
686 (SLT017/20/000100). MS-L is supported by a Miguel Servet contract from the ISCIII Spanish
687 Health Institute (CPII22/00007) and co-financed by the European Social Fund. DD was funded
688 by a Tenovus Scotland Research PhD studentship, T19-06.

689 Author's contributions:

690 AV, MC, and MS-L conceived and designed the study. BS, JD, OP, LC, LN and J-RE generated the
691 clinical database and supplied the samples. GT-S and DD performed the analyses. GT-S, AB, AV,
692 MC, and MS-L interpreted the results. GT-S, AV, MC, and MS-L wrote the manuscript. All
693 authors read and approved the final manuscript.

694 Acknowledgments:

695 We acknowledge the AAA patients at *Hospital de la Santa Creu i Sant Pau* and *Hospital del Mar*
696 who participated in this study, and the multiorgan donor families who made this research
697 possible through their generous consent.

698 Author's information:

699 AV, MC, and MS-L contributed equally to this work as senior authors.

700 **REFERENCES**

- 701 1. Aggarwal S, Qamar A, Sharma V, Sharma A. Abdominal aortic aneurysm: A
702 comprehensive review. *Exp Clin Cardiol* 2011;16:11–5.
- 703 2. Kuivaniemi H, Ryer EJ, Elmore JR, Tromp G. Understanding the pathogenesis of abdominal
704 aortic aneurysms. *Expert Review of Cardiovascular Therapy* 2015;13:975–87.
- 705 3. Holmes DR, Liao S, Parks WC, Thompson RW. Medial neovascularization in abdominal
706 aortic aneurysms: a histopathologic marker of aneurysmal degeneration with
707 pathophysiologic implications. *J Vasc Surg* 1995;21:761–71; discussion 771-772.

- 708 4. Robinson WP, Schanzer A, Li Y, Goodney PP, Nolan BW, Eslami MH, et al. Derivation and
709 validation of a practical risk score for prediction of mortality after open repair of ruptured
710 abdominal aortic aneurysms in a U.S. regional cohort and comparison to existing scoring
711 systems. *J Vasc Surg* 2013;57:354–61.
- 712 5. Chaikof EL, Dalman RL, Eskandari MK, Jackson BM, Lee WA, Mansour MA, et al. The
713 Society for Vascular Surgery practice guidelines on the care of patients with an abdominal
714 aortic aneurysm. *Journal of Vascular Surgery* 2018;67:2-77.e2.
- 715 6. Lederle FA, Johnson GR, Wilson SE, Chute EP, Hye RJ, Makaroun MS, et al. The Aneurysm
716 Detection and Management Study Screening Program: Validation Cohort and Final
717 Results. *Archives of Internal Medicine* 2000;160:1425–30.
- 718 7. Roychowdhury T, Klarin D, Levin MG, Spin JM, Rhee YH, Deng A, et al. Genome-wide
719 association meta-analysis identifies risk loci for abdominal aortic aneurysm and highlights
720 PCSK9 as a therapeutic target. *Nat Genet* 2023;55:1831–42.
- 721 8. Lowe R, Shirley N, Bleackley M, Dolan S, Shafee T. Transcriptomics technologies. *PLoS*
722 *Comput Biol* 2017;13:e1005457.
- 723 9. Wang Z, Gerstein M, Snyder M. RNA-Seq: a revolutionary tool for transcriptomics. *Nat*
724 *Rev Genet* 2009;10:57–63.
- 725 10. Biros E, Gäbel G, Moran CS, Schreurs C, Lindeman JHN, Walker PJ, et al. Differential gene
726 expression in human abdominal aortic aneurysm and aortic occlusive disease. *Oncotarget*
727 2015;6:12984–96.
- 728 11. Lenk GM, Tromp G, Weinsheimer S, Gatalica Z, Berguer R, Kuivaniemi H. Whole genome
729 expression profiling reveals a significant role for immune function in human abdominal
730 aortic aneurysms. *BMC Genomics* 2007;8:237.
- 731 12. Biros E, Moran CS, Rush CM, Gäbel G, Schreurs C, Lindeman JHN, et al. Differential gene
732 expression in the proximal neck of human abdominal aortic aneurysm. *Atherosclerosis*
733 2014;233:211–8.
- 734 13. Choke E, Cockerill GW, Laing K, Dawson J, Wilson WRW, Loftus IM, et al. Whole Genome-
735 expression Profiling Reveals a Role for Immune and Inflammatory Response in Abdominal
736 Aortic Aneurysm Rupture. *European Journal of Vascular and Endovascular Surgery*
737 2009;37:305–10.
- 738 14. Gäbel G, Northoff BH, Weinzierl I, Ludwig S, Hinterseher I, Wilfert W, et al. Molecular
739 Fingerprint for Terminal Abdominal Aortic Aneurysm Disease. *J Am Heart Assoc*
740 2017;6:e006798.
- 741 15. Lindquist Liljeqvist M, Hultgren R, Bergman O, Villard C, Kronqvist M, Eriksson P, et al.
742 Tunica-Specific Transcriptome of Abdominal Aortic Aneurysm and the Effect of
743 Intraluminal Thrombus, Smoking, and Diameter Growth Rate. *Arteriosclerosis,*
744 *Thrombosis, and Vascular Biology* 2020;40:2700–13.
- 745 16. The GTEx Consortium atlas of genetic regulatory effects across human tissues. *Science*
746 2020;369:1318–30.

- 747 17. Márquez-Sánchez AC, Koltsova EK. Immune and inflammatory mechanisms of abdominal
748 aortic aneurysm. *Front Immunol* 2022;13:989933.
- 749 18. Yuan Z, Lu Y, Wei J, Wu J, Yang J, Cai Z. Abdominal Aortic Aneurysm: Roles of Inflammatory
750 Cells. *Frontiers in Immunology [Internet]* 2021 [cited 2022 Jan 25];11. Available from:
751 <https://www.frontiersin.org/article/10.3389/fimmu.2020.609161>
- 752 19. Nie H, Qiu J, Wen S, Zhou W. Combining Bioinformatics Techniques to Study the Key
753 Immune-Related Genes in Abdominal Aortic Aneurysm. *Front Genet* 2020;11:579215.
- 754 20. Hasimbegovic E, Schweiger V, Kastner N, Spannbaauer A, Traxler D, Lukovic D, et al.
755 Alternative Splicing in Cardiovascular Disease—A Survey of Recent Findings. *Genes (Basel)*
756 2021;12:1457.
- 757 21. Rotival M, Quach H, Quintana-Murci L. Defining the genetic and evolutionary architecture
758 of alternative splicing in response to infection. *Nat Commun* 2019;10:1671.
- 759 22. Romero JP, Ortiz-Estévez M, Muniategui A, Carrancio S, de Miguel FJ, Carazo F, et al.
760 Comparison of RNA-seq and microarray platforms for splice event detection using a cross-
761 platform algorithm. *BMC Genomics* 2018;19:703.
- 762 23. Ouyang M, Wang M, Yu B. Aberrant Mitochondrial Dynamics: An Emerging Pathogenic
763 Driver of Abdominal Aortic Aneurysm. *Cardiovasc Ther* 2021;2021:6615400.
- 764 24. Summerhill VI, Sukhorukov VN, Eid AH, Nedosugova LV, Sobenin IA, Orekhov AN.
765 Pathophysiological Aspects of the Development of Abdominal Aortic Aneurysm with a
766 Special Focus on Mitochondrial Dysfunction and Genetic Associations. *Biomolecular*
767 *Concepts* 2021;12:55–67.
- 768 25. Chistiakov DA, Shkurat TP, Melnichenko AA, Grechko AV, Orekhov AN. The role of
769 mitochondrial dysfunction in cardiovascular disease: a brief review. *Annals of Medicine*
770 2018;50:121–7.
- 771 26. Leeper NJ, Tedesco MM, Kojima Y, Schultz GM, Kundu RK, Ashley EA, et al. Apelin
772 prevents aortic aneurysm formation by inhibiting macrophage inflammation. *American*
773 *Journal of Physiology-Heart and Circulatory Physiology* 2009;296:H1329–35.
- 774 27. Shin SJ, Hang HT, Thang BQ, Shimoda T, Sakamoto H, Osaka M, et al. Role of PAR1-Egr1 in
775 the Initiation of Thoracic Aortic Aneurysm in Fbln4-Deficient Mice. *Arteriosclerosis,*
776 *Thrombosis, and Vascular Biology* 2020;40:1905–17.
- 777 28. Wang S, Liu H, Yang P, Wang Z, Ye P, Xia J, et al. A role of inflammaging in aortic aneurysm:
778 new insights from bioinformatics analysis. *Frontiers in Immunology [Internet]* 2023 [cited
779 2023 Dec 17];14. Available from:
780 <https://www.frontiersin.org/articles/10.3389/fimmu.2023.1260688>
- 781 29. Sung PH, Yang YH, Chiang HJ, Chiang JY, Chen CJ, Liu CT, et al. Risk of aortic aneurysm and
782 dissection in patients with autosomal-dominant polycystic kidney disease: a nationwide
783 population-based cohort study. *Oncotarget* 2017;8:57594–604.
- 784 30. Kugo H, Moriyama T, Zaima N. The role of perivascular adipose tissue in the appearance
785 of ectopic adipocytes in the abdominal aortic aneurysmal wall. *Adipocyte* 2019;8:229–39.

- 786 31. Chislock EM, Pendergast AM. Abl Family Kinases Regulate Endothelial Barrier Function In
787 Vitro and in Mice. *PLoS One* 2013;8:e85231.
- 788 32. Beghi S, Furmanik M, Jaminon A, Veltrop R, Rapp N, Wichapong K, et al. Calcium
789 Signalling in Heart and Vessels: Role of Calmodulin and Downstream Calmodulin-
790 Dependent Protein Kinases. *Int J Mol Sci* 2022;23:16139.
- 791 33. Bround MJ, Wambolt R, Luciani DS, Kulpa JE, Rodrigues B, Brownsey RW, et al.
792 Cardiomyocyte ATP Production, Metabolic Flexibility, and Survival Require Calcium Flux
793 through Cardiac Ryanodine Receptors in Vivo. *J Biol Chem* 2013;288:18975–86.
- 794 34. Colotti G, Poser E, Fiorillo A, Genovese I, Chiarini V, Ilari A. Sorcin, a Calcium Binding
795 Protein Involved in the Multidrug Resistance Mechanisms in Cancer Cells. *Molecules*
796 2014;19:13976–89.
- 797 35. Sanders KM. Invited Review: Mechanisms of calcium handling in smooth muscles.
798 *Journal of Applied Physiology* 2001;91:1438–49.
- 799 36. Wang K, Wei G, Liu D. CD19: a biomarker for B cell development, lymphoma diagnosis
800 and therapy. *Experimental Hematology & Oncology* 2012;1:36.
- 801 37. Zhang L, Wang Y. B lymphocytes in abdominal aortic aneurysms. *Atherosclerosis*
802 2015;242:311–7.
- 803 38. Forester ND, Cruickshank SM, Scott DJA, Carding SR. Functional characterization of T cells
804 in abdominal aortic aneurysms. *Immunology* 2005;115:262–70.
- 805 39. Sagan A, Mikolajczyk TP, Mrowiecki W, MacRitchie N, Daly K, Meldrum A, et al. T Cells Are
806 Dominant Population in Human Abdominal Aortic Aneurysms and Their Infiltration in the
807 Perivascular Tissue Correlates With Disease Severity. *Frontiers in Immunology* [Internet]
808 2019 [cited 2024 Feb 9];10. Available from:
809 <https://www.frontiersin.org/journals/immunology/articles/10.3389/fimmu.2019.01979>
- 810 40. Xiong T, Lv XS, Wu GJ, Guo YX, Liu C, Hou FX, et al. Single-Cell Sequencing Analysis and
811 Multiple Machine Learning Methods Identified GOS2 and HPSE as Novel Biomarkers for
812 Abdominal Aortic Aneurysm. *Front Immunol* 2022;13:907309.
- 813 41. Ferreira PG, Muñoz-Aguirre M, Reverter F, Sá Godinho CP, Sousa A, Amadoz A, et al. The
814 effects of death and post-mortem cold ischemia on human tissue transcriptomes. *Nat*
815 *Commun* 2018;9:490.
- 816 42. Forester ND, Cruickshank SM, Scott DJA, Carding SR. Increased natural killer cell activity in
817 patients with an abdominal aortic aneurysm. *British Journal of Surgery* 2006;93:46–54.
- 818 43. Golledge J, Muller J, Shephard N, Clancy P, Smallwood L, Moran C, et al. Association
819 Between Osteopontin and Human Abdominal Aortic Aneurysm. *Arteriosclerosis,*
820 *Thrombosis, and Vascular Biology* 2007;27:655–60.
- 821 44. Black KM, Masuzawa A, Hagberg RC, Khabbaz KR, Trovato ME, Rettagliati VM, et al.
822 Preliminary Biomarkers for Identification of Human Ascending Thoracic Aortic Aneurysm.
823 *J Am Heart Assoc* 2013;2:e000138.

- 824 45. Icer MA, Gezmen-Karadag M. The multiple functions and mechanisms of osteopontin.
825 Clinical Biochemistry 2018;59:17–24.
- 826 46. Wang SK, Green LA, Gutwein AR, Gupta AK, Babbey CM, Motaganahalli RL, et al.
827 Osteopontin may be a driver of abdominal aortic aneurysm formation. Journal of Vascular
828 Surgery 2018;68:225-295.
- 829 47. Liu H, Zhang Y, Song W, Sun Y, Jiang Y. Osteopontin N-Terminal Function in an Abdominal
830 Aortic Aneurysm From Apolipoprotein E-Deficient Mice. Frontiers in Cell and
831 Developmental Biology [Internet] 2021 [cited 2023 Nov 22];9. Available from:
832 <https://www.frontiersin.org/articles/10.3389/fcell.2021.681790>
- 833 48. Qin X, He L, Tian M, Hu P, Yang J, Lu H, et al. Smooth muscle-specific G α deletion
834 exaggerates angiotensin II-induced abdominal aortic aneurysm formation in mice in vivo.
835 J Mol Cell Cardiol 2019;132:49–59.
- 836 49. Zhang R, Ji Z, Yao Y, Zuo W, Yang M, Qu Y, et al. Identification of hub genes in unstable
837 atherosclerotic plaque by conjoint analysis of bioinformatics. Life Sciences
838 2020;262:118517.
- 839 50. Greene D, Pirri D, Frudd K, Sackey E, Al-Owain M, Giese APJ, et al. Genetic association
840 analysis of 77,539 genomes reveals rare disease etiologies. Nat Med 2023;29:679–88.
- 841 51. Kobeissi E, Hibino M, Pan H, Aune D. Blood pressure, hypertension and the risk of
842 abdominal aortic aneurysms: a systematic review and meta-analysis of cohort studies.
843 Eur J Epidemiol 2019;34:547–55.
- 844 52. Wang B, Cai W, Ai D, Zhang X, Yao L. The Role of Deubiquitinases in Vascular Diseases. J. of
845 Cardiovasc. Trans. Res. 2020;13:131–41.
- 846 53. Johnson M. Molecular mechanisms of β 2-adrenergic receptor function, response, and
847 regulation. Journal of Allergy and Clinical Immunology 2006;117:18–24.
- 848 54. Ding T, Zhou Y, Long R, Chen C, Zhao J, Cui P, et al. DUSP8 phosphatase: structure,
849 functions, expression regulation and the role in human diseases. Cell & Bioscience
850 2019;9:70.
- 851 55. Baldo G, Wu S, Howe RA, Ramamoothy M, Knutsen RH, Fang J, et al. Pathogenesis of
852 aortic dilatation in mucopolysaccharidosis VII mice may involve complement activation.
853 Mol Genet Metab 2011;104:608–19.
- 854 56. Emery P, Durand B, Mach B, Reith W. RFX proteins, a novel family of DNA binding proteins
855 conserved in the eukaryotic kingdom. Nucleic Acids Res 1996;24:803–7.
- 856 57. Liu Y, Wang X, Wang H, Hu T. Identification of key genes and pathways in abdominal aortic
857 aneurysm by integrated bioinformatics analysis. J Int Med Res
858 2020;48:0300060519894437.
- 859 58. Du P, Gao K, Cao Y, Yang S, Wang Y, Guo R, et al. RFX1 downregulation contributes to TLR4
860 overexpression in CD14+ monocytes via epigenetic mechanisms in coronary artery
861 disease. Clin Epigenetics 2019;11:44.

- 862 59. Blomkalns AL, Gavrilu D, Thomas M, Neltner BS, Blanco VM, Benjamin SB, et al. CD14
863 Directs Adventitial Macrophage Precursor Recruitment: Role in Early Abdominal Aortic
864 Aneurysm Formation. *J Am Heart Assoc* 2013;2:e000065.
- 865 60. An imprinted, mammalian bicistronic transcript encodes two independent proteins |
866 PNAS [Internet]. [cited 2024 Feb 12];Available from:
867 <https://www.pnas.org/doi/10.1073/pnas.96.10.5616>
- 868 61. Zhang K, Li M, Yin L, Fu G, Liu Z. Role of thrombospondin-1 and thrombospondin-2 in
869 cardiovascular diseases (Review). *Int J Mol Med* 2020;45:1275–93.
- 870 62. Liu Z, Morgan S, Ren J, Wang Q, Annis DS, Mosher DF, et al. Thrombospondin-1 (TSP1)
871 Contributes to the Development of Vascular Inflammation by Regulating Monocytic Cell
872 Motility in Mouse Models of Abdominal Aortic Aneurysm. *Circulation Research*
873 2015;117:129–41.
- 874 63. Wang C, Gong B, Bushel PR, Thierry-Mieg J, Thierry-Mieg D, Xu J, et al. A comprehensive
875 study design reveals treatment- and transcript abundance–dependent concordance
876 between RNA-seq and microarray data. *Nat Biotechnol* 2014;32:926–32.
- 877 64. Dobin A, Davis CA, Schlesinger F, Drenkow J, Zaleski C, Jha S, et al. STAR: ultrafast
878 universal RNA-seq aligner. *Bioinformatics* 2013;29:15–21.
- 879 65. Li B, Dewey CN. RSEM: accurate transcript quantification from RNA-Seq data with or
880 without a reference genome. *BMC Bioinformatics* 2011;12:323.
- 881 66. Harrow J, Frankish A, Gonzalez JM, Tapanari E, Diekhans M, Kokocinski F, et al. GENCODE:
882 The reference human genome annotation for The ENCODE Project. *Genome Res*
883 2012;22:1760–74.
- 884 67. Benjamini Y, Hochberg Y. Controlling the False Discovery Rate: A Practical and Powerful
885 Approach to Multiple Testing. *Journal of the Royal Statistical Society: Series B*
886 (Methodological) 1995;57:289–300.
- 887 68. Yu G, Wang LG, Han Y, He QY. clusterProfiler: an R Package for Comparing Biological
888 Themes Among Gene Clusters. *OMICS* 2012;16:284–7.
- 889 69. Subramanian A, Tamayo P, Mootha VK, Mukherjee S, Ebert BL, Gillette MA, et al. Gene set
890 enrichment analysis: A knowledge-based approach for interpreting genome-wide
891 expression profiles. *Proceedings of the National Academy of Sciences* 2005;102:15545–
892 50.
- 893 70. KEGG: new perspectives on genomes, pathways, diseases and drugs | *Nucleic Acids*
894 *Research* | Oxford Academic [Internet]. [cited 2023 Apr 27];Available from:
895 <https://academic.oup.com/nar/article/45/D1/D353/2605697>
- 896 71. Storey JD. A Direct Approach to False Discovery Rates. *Journal of the Royal Statistical*
897 *Society. Series B (Statistical Methodology)* 2002;64:479–98.
- 898 72. Kersevicute I, Gordevicius J. aPEAR: an R package for autonomous visualization of
899 pathway enrichment networks. *Bioinformatics* 2023;39:btad672.

- 900 73. Yu G, Hu E, Gao CH. enrichplot: Visualization of Functional Enrichment Result [Internet].
901 2023 [cited 2023 Nov 21]; Available from: <https://bioconductor.org/packages/enrichplot/>
- 902 74. Chen B, Khodadoust MS, Liu CL, Newman AM, Alizadeh AA. Profiling tumor infiltrating
903 immune cells with CIBERSORT. *Methods Mol Biol* 2018;1711:243–59.
- 904 75. Castel SE, Mohammadi P, Chung WK, Shen Y, Lappalainen T. Rare variant phasing and
905 haplotypic expression from RNA sequencing with phASER. *Nat Commun* 2016;7:12817.
- 906 76. Degner JF, Marioni JC, Pai AA, Pickrell JK, Nkadori E, Gilad Y, et al. Effect of read-mapping
907 biases on detecting allele-specific expression from RNA-sequencing data. *Bioinformatics*
908 2009;25:3207–12.
- 909 77. van de Geijn B, McVicker G, Gilad Y, Pritchard JK. WASP: allele-specific software for robust
910 molecular quantitative trait locus discovery. *Nat Methods* 2015;12:1061–3.
- 911 78. Castel SE, Aguet F, Mohammadi P, Aguet F, Anand S, Ardlie KG, et al. A vast resource of
912 allelic expression data spanning human tissues. *Genome Biology* 2020;21:234.
- 913 79. van Beek D, Verdonschot J, Derks K, Brunner H, de Kok TM, Arts ICW, et al. Allele-specific
914 expression analysis for complex genetic phenotypes applied to a unique dilated
915 cardiomyopathy cohort. *Sci Rep* 2023;13:564.

916 **FIGURE LEGENDS**

917 **Figure 1**

918 Study design flowchart.

919 **Figure 2**

920 Hierarchical clustering analysis results with all the DEGs between AAA and controls (A) and
921 after removing DEG by ischemic time (B). C) Comparison of the proportion of inflammatory
922 cells between AAA and controls using CIBERSORTx.

923 **Figure 3**

924 A) Significant alternative splicing types identified between AAA and controls. B) Venn diagram
925 showing the overlap between DEGs in AAA and controls and genes with differential alternative
926 splicing patterns in AAA and controls. C) Venn diagram showing the overlap between DEGs in
927 AAA and controls and DEGs by AAA diameter.

928 **Figure 4**

929 A) Results of PC analysis clustering between AAA and controls. B) Hierarchical clustering
930 analysis results with genes with different allelic specific patterns between AAA and controls.

931 **SUPPLEMENTARY INFORMATION**

932 **Additional file 1:** Figures S1-S6

933 Contains Supplementary Figures S1-S6.

934 **Additional file 2:** Table S1

935 Complete differential expression results between AAA and controls.

936 **Additional file 3:** Table S2

937 GO functional enrichment analysis results between AAA and controls (including genes affected
938 by ischemic time).

939 **Additional file 4:** Table S3

940 KEGG functional enrichment analysis results between AAA and controls (including genes
941 affected by ischemic time).

942 **Additional file 5:** Table S4

943 Differential expressed genes by ischemic time in GTEx samples.

944 **Additional file 6:** Table S5

945 GO functional enrichment analysis results between AAA and controls (excluding genes affected
946 by ischemic time).

947 **Additional file 7:** Table S6

948 KEGG functional enrichment analysis results between AAA and controls (excluding genes
949 affected by ischemic time).

950 **Additional file 8:** Table S7

951 Results of the alternative splicing study between AAA and controls.

952 **Additional file 9:** Table S8

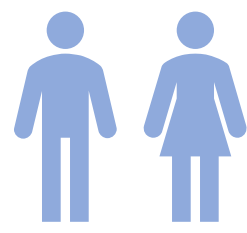
953 Complete differential expression results between AAA of different diameter.

954 **Additional file 10:** Table S9

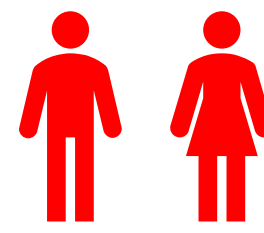
955 Correlation analysis between biological and technical covariates.

TRIPLE A BARCELONA STUDY

Controls
N = 44

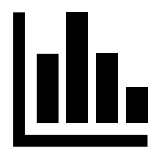


AAA
N = 96



Patients' characteristics

Data analysis



Whole transcriptome sequencing
on aortic tissue samples
N = 140

Alignment: STAR
Genome: GRCh38
Gencode: v26

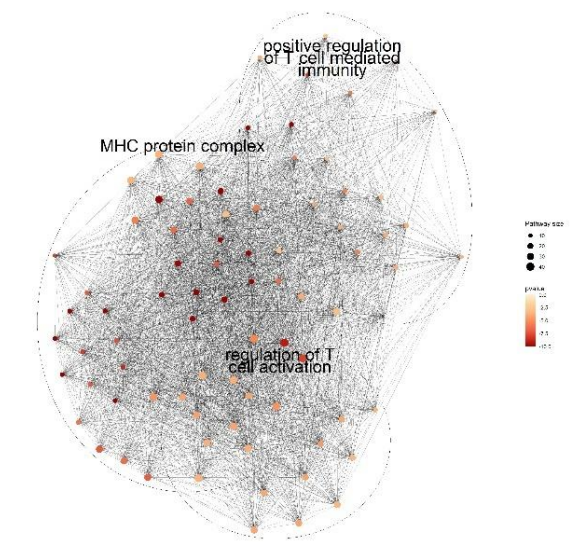
Quantification: RSEM
N^o genes = 36,712

Genotype data on AAA
N = 12

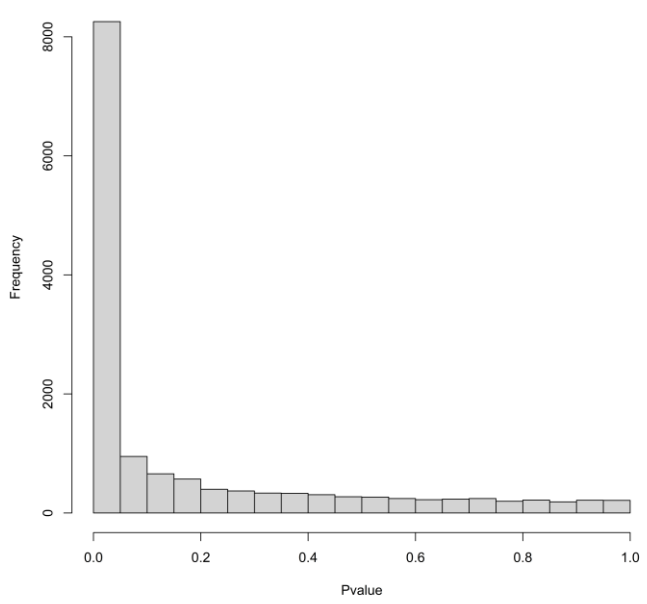
Allelic specific expression

GTEX aortic samples
N = 387

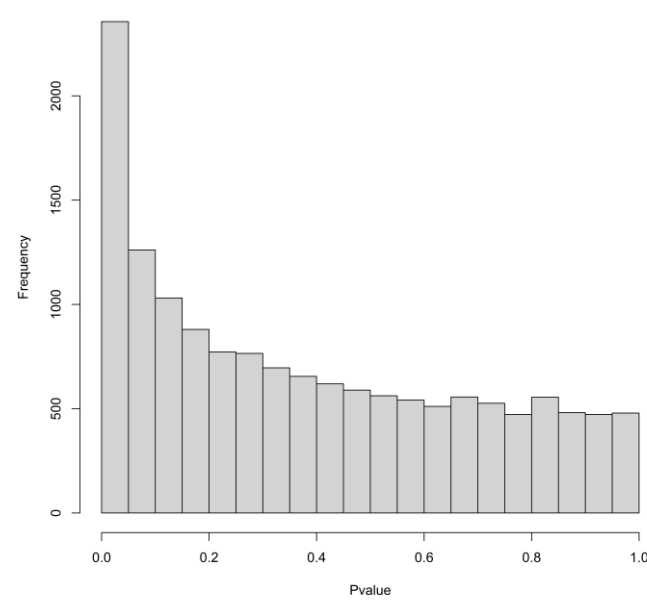
Gene set enrichment analysis
and cluster analysis



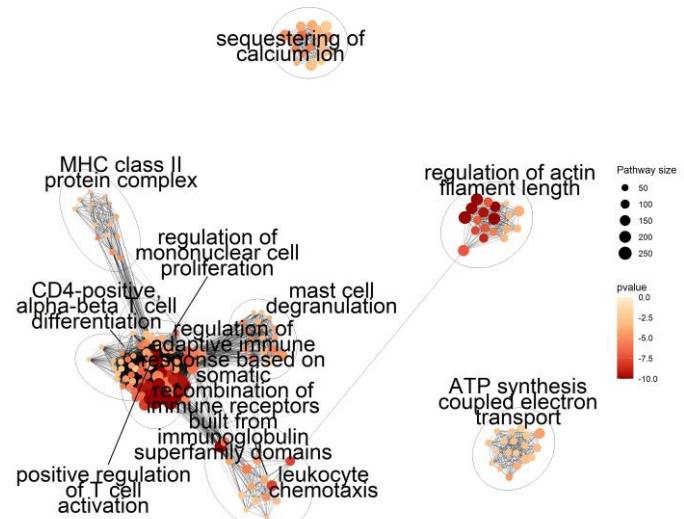
AAA vs Controls



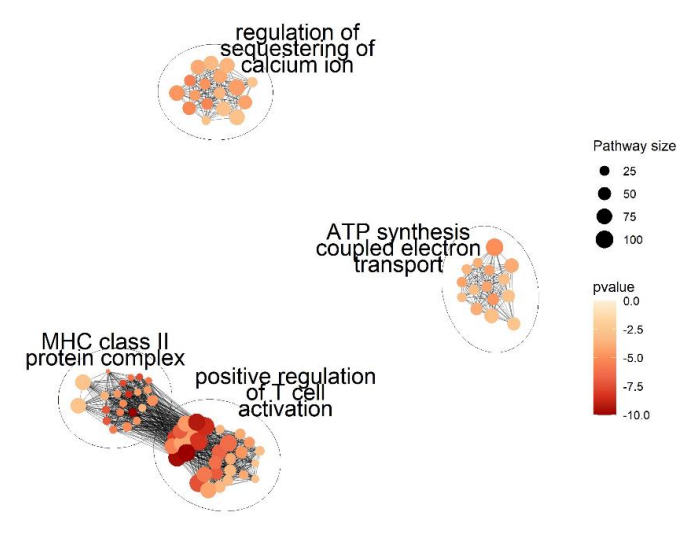
AAA of varying diameter



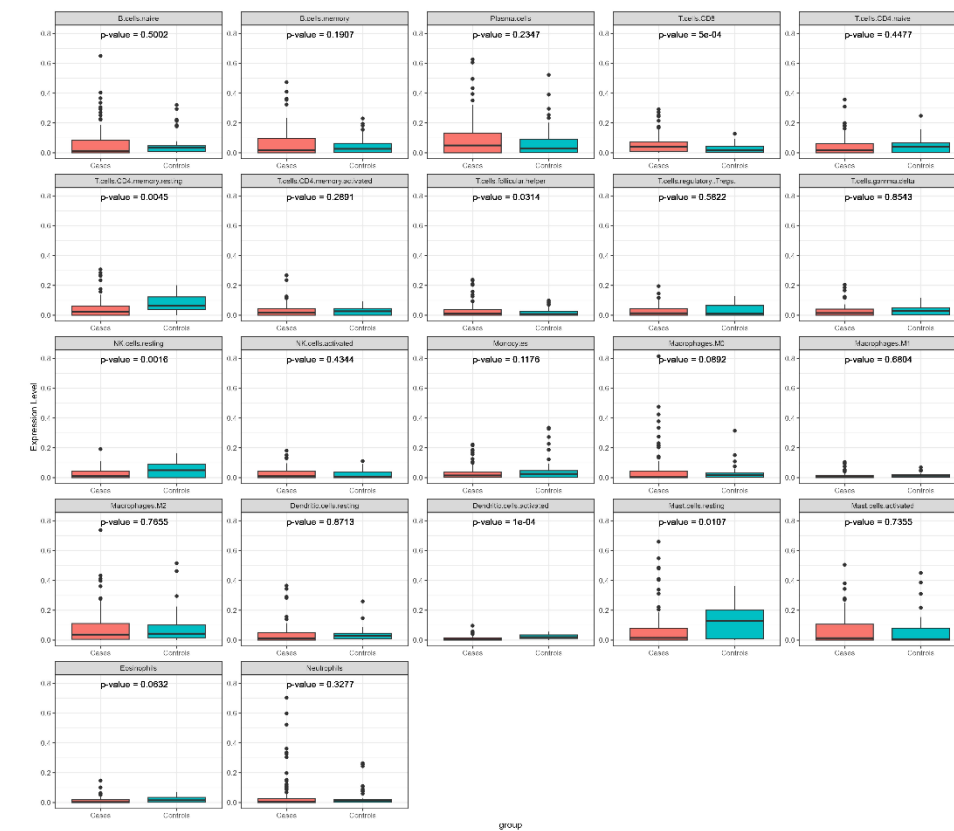
Gene set enrichment analysis
and cluster analysis



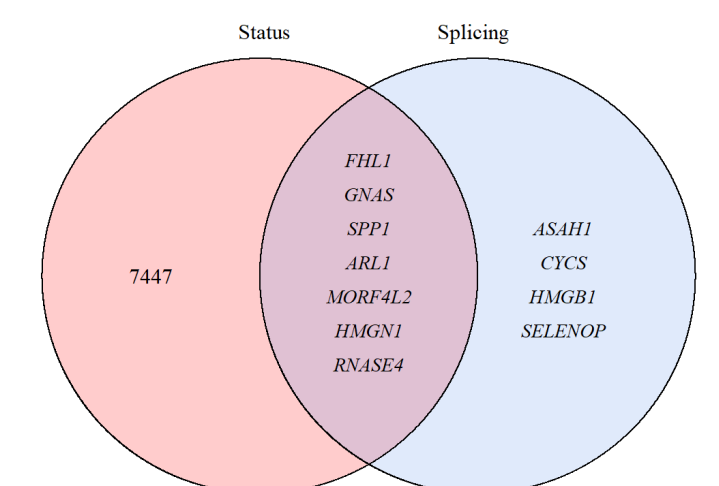
Study effect of ischemic time



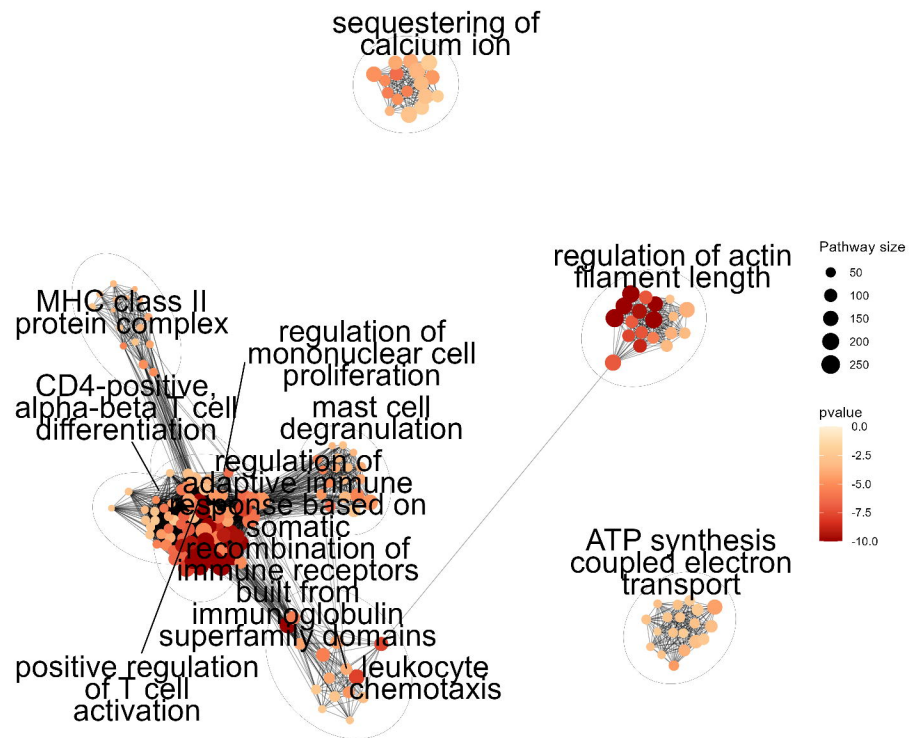
Study of inflammatory infiltrate



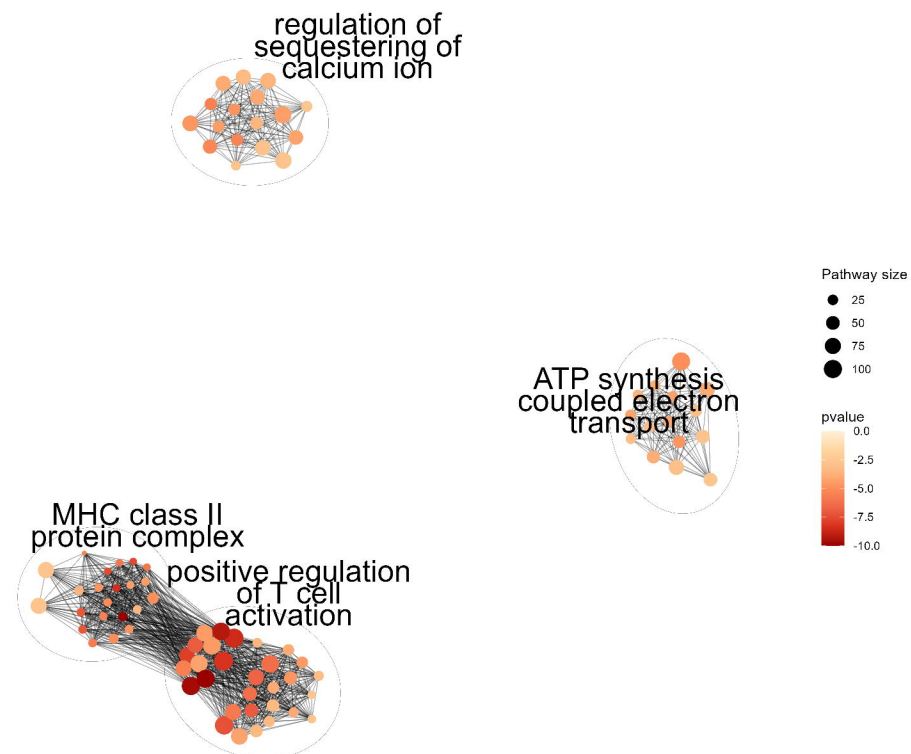
Study of alternative splicing



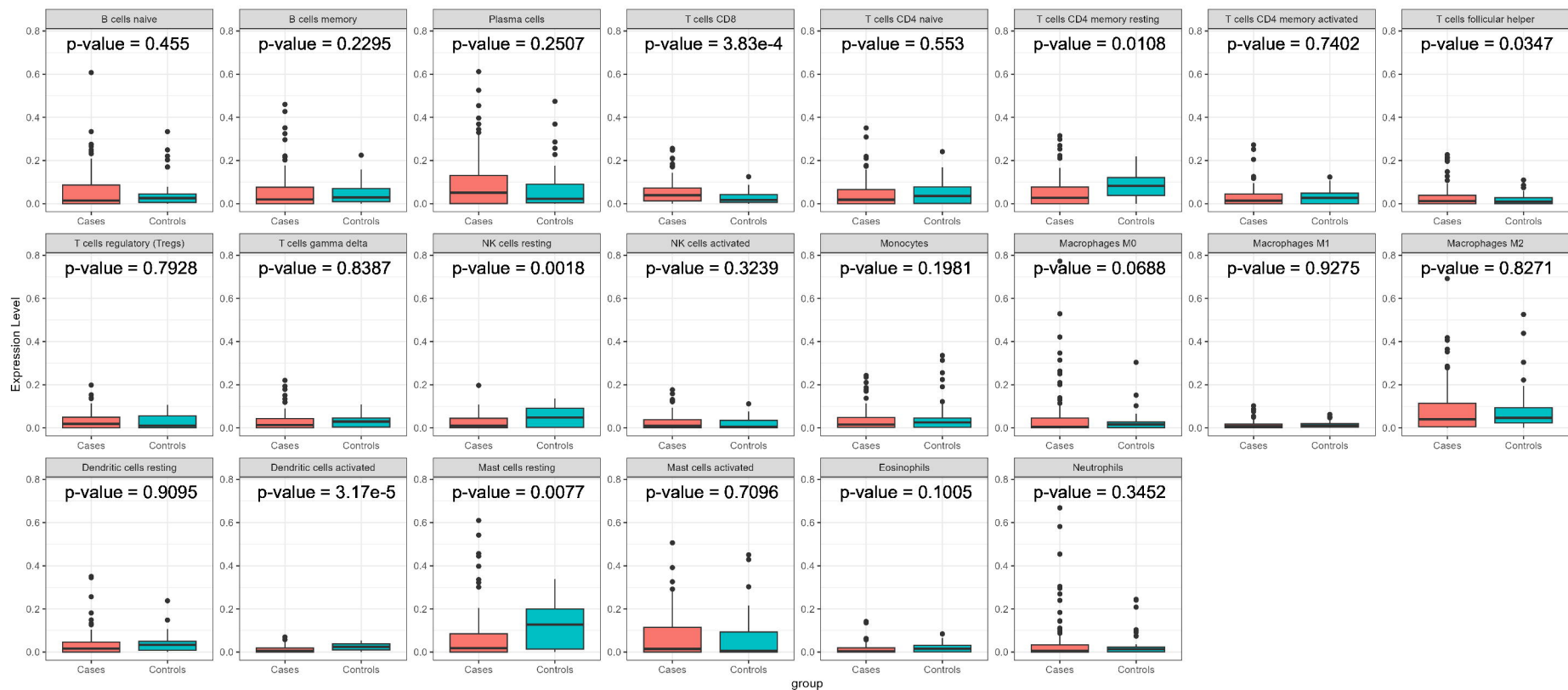
A)



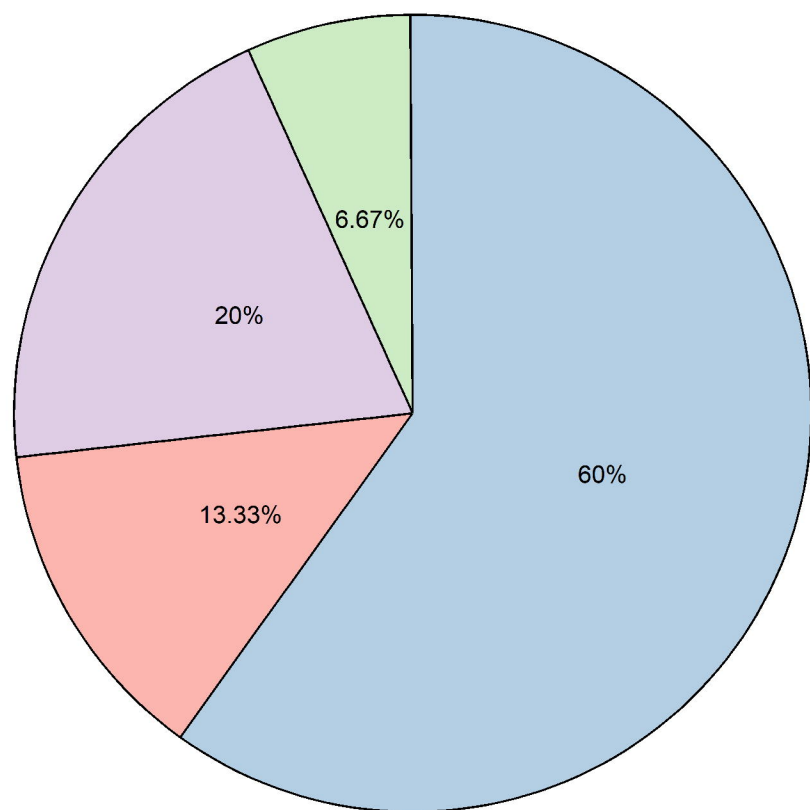
B)



C)

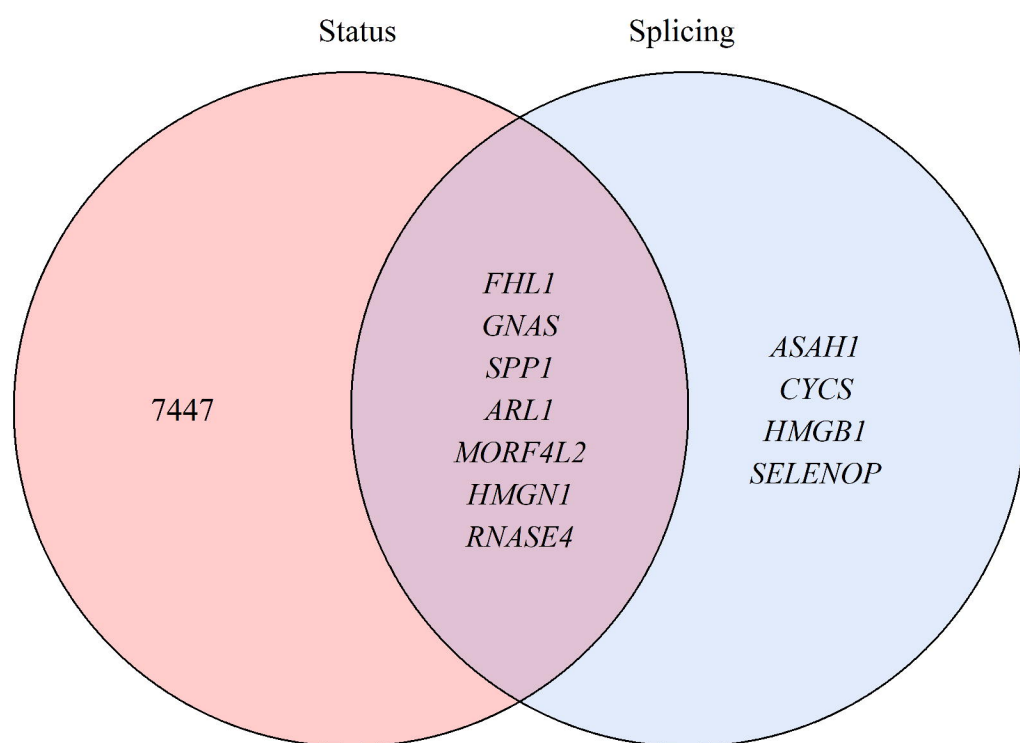


A)

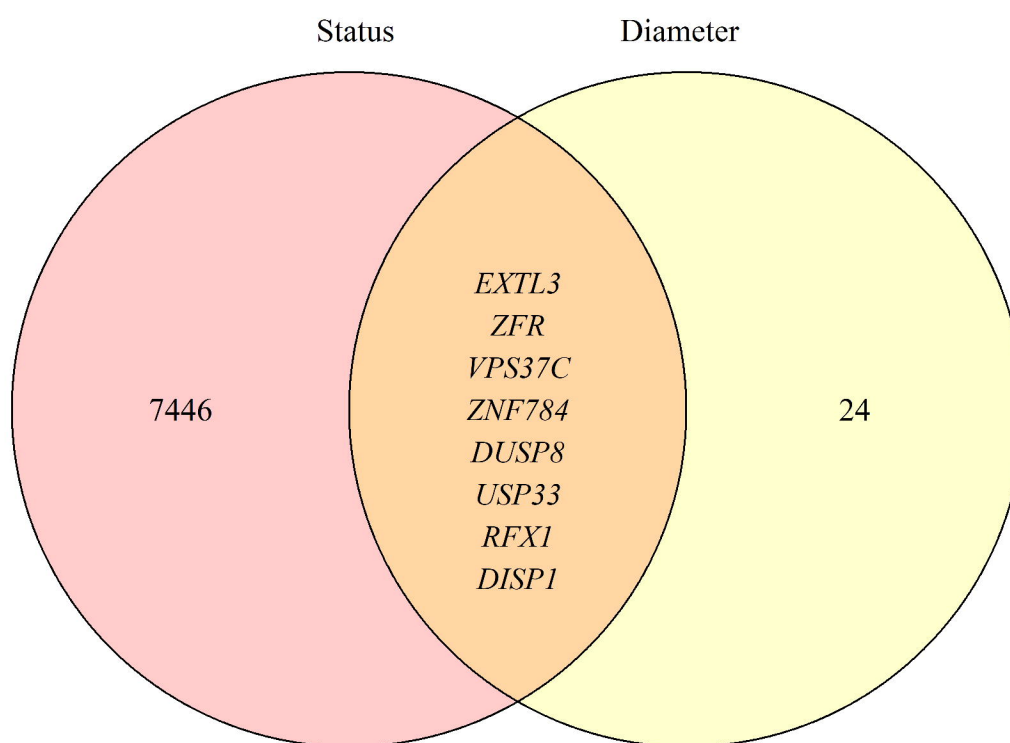


Alternative 5' Splice Site Alternative First Exon
 Mutually Exclusive Exons Skipping Exon

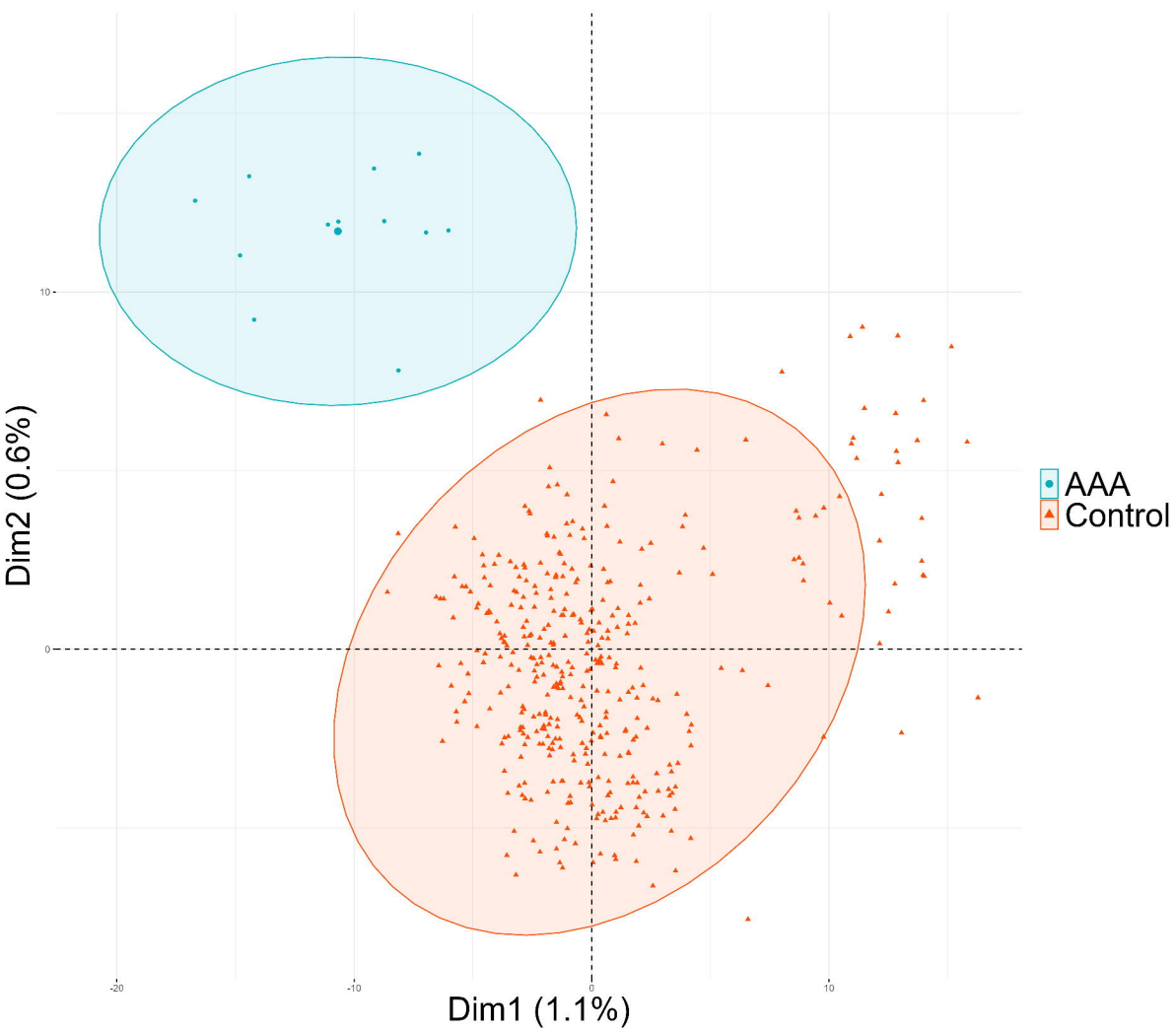
B)



C)



A)



B)

